Towards a sustainable synthesis of aromatic isocyanates : by the palladium diphosphane catalyzed reduction of nitrobenzene; a first step

Mooibroek, T.J.

Chapter 4

Mechanistic study of the palladium–bidentate diarylphosphane catalysed carbonylation of nitrobenzene in methanol; a palladium-imido complex as the central product-releasing species.

Abstract: The L_2Pd^{II} catalyzed reduction of nitrobenzene with CO in methanol was studied using bidentate diphenyl phosphane ligands with different backbone spacers and aryl ring substituents. More carbonylation products (methylphenyl carbamate, diphenyl urea) are formed relative to hydrogenation products (aniline, diphenylurea) when using a ligand with smaller bite–angle (C_3–backbone) or equipping the ligand with *ortho*–methoxy groups. Up to 73% coupling products (azo(xy)benzene) were obtained when using a ligand with a larger bite–angle (C_4–backbone). Based on these observations and the dependencies of the product formation on reactant concentrations ($PhNO_2$, CO) it is proposed that all products compete for the same palladium–imido (P_2Pd^{II}=NPh) intermediate. Additional proof for the existence and reactivity of P_2Pd^{II}=NPh species comes from a $^{31}P\{^1H\}$NMR and ESI–MS analysis of a reaction of a P_2Pd^0 compound with mesityl azide, forming what appears to be a Pd-imido complex. This complex was shown to react with CO and methanol to give methyl mesityl carbamate under mild conditions.

The palladacycle **C7** 'P$_2$PdC(O)N(Ph)OC(O)' was considered as an alternative carbonylation product releasing intermediate. However, ligand exchange reactions of the stable 'phen–**C7**' with diphosphane ligands (studied with $^{31}P\{^1H\}$–NMR and ESI-MS) indicate that the 5–membered 'P$_2$–**C7**' readily decomposes under mild conditions by loss of CO rather than CO_2, to eventually (presumably) form the P_2Pd^{II}=NPh intermediate instead of carbonylation products. DFT calculation indicate that steric repulsion causes the lower stability of a diphosphane–**C7** relative to phen–**C7**.

These combined catalytic and organometallic data thus all point strongly to a P_2Pd^{II}=NPh complex as *the sole most probable product-releasing* intermediate species.

4.1. Introduction

Aromatic isocyanates are useful molecules, and annually produced on the megaton scale.[1] In particular, the polymer precursors MDI and TDI[2, 3] (Figure 4.1) are produced from nitrobenzene in efficient but less–desirable processes.[4] These processes are generally referred to as the 'phosgene routes', as they are based on the usage of the highly toxic[5, 6] phosgene gas (~100 times more toxic than CO).
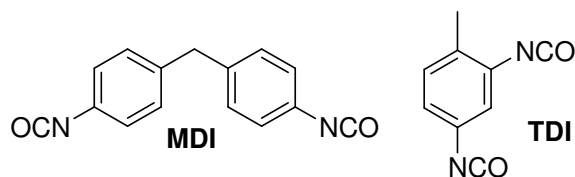
Figure 4.1. Two industrially produced aromatic isocyanates.

The most viable alternative that has emerged so far, is the reductive carbonylation of nitrobenzene with CO, producing only CO_2 as by–product.[7] The often reported aryl–containing side products that can be formed in this reaction comprise the self–coupling products azobenzene (Azo) and azoxybenzene (Azoxy). When this reaction is performed in methanol, methylphenylcarbamate (MPC) is usually the main product, with the co–production of Azo, Azoxy, aniline and/or N,N'–diphenylurea (DPU).[7, 8] MPC can be pyrolyzed to liberate the desired phenylisocyanate, recovering methanol.

It was discovered in the 1980s that palladium(II) stabilized with bidentate N– or P–ligands yields relatively active catalysts for this reaction (~500 turnover numbers, in methanol).[9-11] Most scientific studies have thus far concentrated on studying the $[Pd(phen)_2]X_2$ / H^+ catalytic system in methanol (phen = 1,10–phenanthroline),[8, 12-22] leaving the Pd–phosphorus–based systems virtually unstudied.[19, 23-26] In particular, mechanistic studies have not been reported for such a Pd–phosphorus based system.

Mechanistic proposals for the reaction catalyzed by Pd–phen systems generally start with oxidative coupling of CO and $PhNO_2$ at an (*in situ* generated) Pd^0 species to form a Pd^{II} species.[7, 20, 27] During the proposed catalytic cycle the catalyst remains in the Pd^{II} oxidation state, but in the final MPC–generating step

Pd^0 is regenerated from a palladacyclic intermediate such as the one shown in Figure 4.2a. [7, 16, 18, 20, 28, 29]

Speculations about the intermediacy of palladium–imido compounds (see Figure 4.2b) in catalytic reactions have been put forward in literature of the 1960's and 1970's. Their existence has been postulated in the context of nitrobenzene reduction to aniline with CO/H_2O,[30, 31] in the carbonylation of nitrobenzene to phenylisocyanate,[32, 33] and also

Figure 4.2. Two complexes that could be intermediates in the reductive carbonylation of nitrobenzene: (a) palladacyclic complex, and (b) palladium–imido complex. L_2 = chelating bidentate ligand.

speculatively proposed in the palladium/phen/acid catalyzed nitrobenzene carbonylation in methanol as the reaction medium.[20, 27] It has been proposed that the palladium-catalyzed reduction of functionalized nitroarenes with CO proceeds *via* a palladium–imido intermediate to yield N-heterocyclic compounds.[34, 35] A series of bidentate phosphane stabilized Ni–imido complexes has been isolated, characterized crystallographically, and were shown to react with CO to form isocyanates.[36-38]

One of the most remarkable observations during the catalytic nitrobenzene carbonylation studies using Pd–bidentate diarylphosphane catalyst precursors (Chapter 3), concerned the significant co–production of various methanol oxidation products.[39] These products include dimethyl carbonate (DMC), dimethyl oxalate (DMO), methyl formate (MF), and even carbon monoxide (CO). The H–atoms that are liberated during these methanol oxidation processes are transferred to nitrobenzene and are found back in the products $PhNH_2$, DPU and H_2O. A palladacyclic species such as depicted in Figure 4.2a cannot be used to rationalize the formation of oxidation products of methanol, nor can it be used to explain the H–transfer process from methanol to nitrobenzene. It was therefore proposed (see also Chapter 3) that a Pd–imido complex (Figure 4.2b) must be a key–intermediate species in the catalytic system, as it allows for a clear catalytic connection to be made between the oxidation of methanol and the reduction of

109

nitrobenzene.[39] Starting from such an imido complex, the formation of *all* aryl–containing reaction products commonly observed (i.e., MPC, DPU, Azo(xy)benzene and $PhNH_2$) can be easily rationalized, whereas a palladacyclic species can only explain the formation of nitrobenzene carbonylation products (MPC and DPU, or 'PhNCO' in general). Some evidence for the intermediacy of palladium–imide complexes in the present catalytic system came from trapping experiments, which showed formation of 7–phenyl–7–aza–bicyclo[4.1.0]heptane when carbonylation of nitrobenzene was carried out in the presence of cyclohexene.[39]

In the present mechanistic study, a variety of bidentate diarylphosphane ligands have been used with variation in the length and rigidity of the backbone spacer, and with different substituents on the aryl rings with the aim to differentiate between electronic and steric effects of the ligands on the product distribution. Additional mechanistic information has been gathered from studying the effects of reaction conditions on the product composition. Finally, efforts were undertaken aimed at the development of synthetic routes to the proposed palladacyclic and palladium–imido complexes and to investigate their fate with NMR and ESI–MS characterization techniques, as well as with DFT calculations.

4.2. Results

4.2.1. General considerations

It was shown in Chapter 2 that complex formation of $Pd(OAc)_2$ with the ligands used in this study, yielding $P_2Pd(OAc)_2$, is instantaneous in methanol.[40] Therefore, the catalyst precursor $P_2Pd(OAc)_2$ in the catalytic studies was formed *in situ* from $Pd(OAc)_2$ and the bidentate ligand (1:1.5). The relatively small excess of ligand 'P_2' over the stoichiometric amount of Pd was applied to allow rapid quantitative formation of $P_2Pd(OAc)_2$. A small excess of ligand is also required to compensate for small amounts of mono–phosphane oxide impurities or the formation of small amounts of phosphane oxide during the reaction. Reproducible catalytic results with *in situ* formed catalysts, obtained at the ratio $P_2/Pd=1.5$, were found to be indistinguishable from those of preformed $P_2Pd(OAc)_2$ complexes.

The products that are formed during a catalytic experiment are shown in Scheme 4.1. The aryl-containing reduction products of nitrobenzene can be grouped in carbonylation products methylphenylcarbamate (MPC) and *N,N'*diphenylurea (DPU), coupling products azobenzene (Azo) and azoxybenzene (Azoxy), and hydrogenation products aniline (PhNH$_2$) and DPU.[41] The formation of PhNH$_2$ and DPU requires a source of H–atoms. In the present system methanol is the primary H–source by acting as transfer hydrogenation agent for nitrobenzene.[39] These methanol oxidation processes lead to the formation of the oxidative carbonylation products dimethyl carbonate (DMC), dimethyl oxalate (DMO), and to the formation of oxidative dehydrogenation products methyl formate (MF), water, and carbon monoxide.
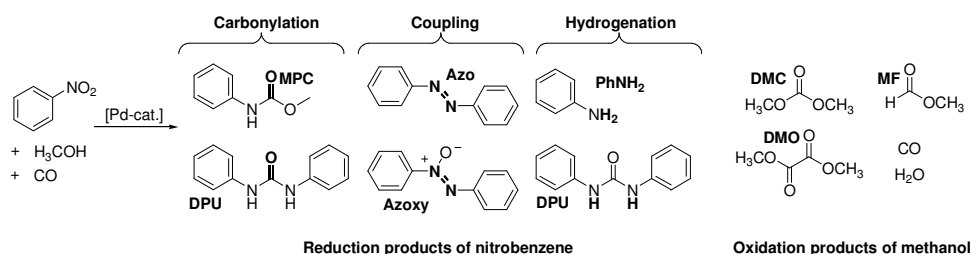
Scheme 4.1. Overview of the different products that are formed in the palladium–catalyzed carbonylation of nitrobenzene in methanol.

The stability of the aryl–containing reaction products was tested under standard catalytic conditions (Table AIII.2) and in all cases except one, these products were found to be inert. The exception is DPU, which reacts with methanol to form MPC and aniline with about 50% conversion (4 hours at 110 ℃). Note that DPU can thus be seen as consisting of 'phenylisocyanate' (carbonylation product) and 'aniline' (hydrogenation product). It is therefore best to view both MPC and DPU *together* as carbonylation products, and aniline and DPU *together* as hydrogenation products. The coupling products Azo and Azoxy were detected with most catalysts; Azoxy is always the major product with selectivity up to 70% while Azo is a minor product (<5%).

In the initial catalyst screening studies a large variety of diarylphosphane ligands has been used. The observed trends in the different reactivity and selectivities will be discussed using the ligands shown in Figure 4.3. These ligands have either a

propylene (L3) or a butylene (L4) backbone, which is in some cases made more rigid by substitution (indicated by 'X'). The aryl rings of the ligands were functionalized with methoxy groups in the *ortho* or *para* position (oMeO– or pMeO–) in order to differentiate between steric and electronic effects.

L3	(R=H)	L4	(R=H)
L3X	(R=H)	L4X	(R=H)
oMeO–L3	(R=o–MeO)		
oMeO–L3X	(R=o–MeO)	oMeO–L4X	(R=o–MeO)
pMeO–L3	(R=p–MeO)	pMeO–L4X	(R=p–MeO)
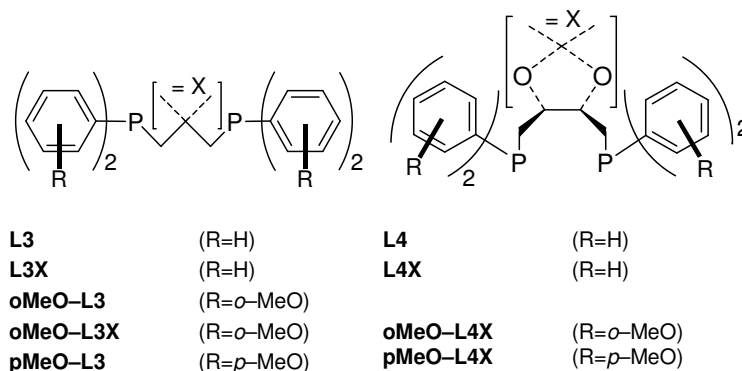
Figure 4.3. The ligands used in the catalytic experiments reported in this study.

The focus of the present chapter is the study of the influence of catalyst structure and carbonylation conditions on the formation of the various aryl–containing reduction products of nitrobenzene, and the possible role of a palladacyclic– and/or palladium imido–complex (Figure 4.2b) as intermediate in the formation of these products. Therefore, only the data of aryl–containing reaction products are shown in Table 4.1. A full analysis of the reaction mixtures was always performed however, and the data of the other reaction products are available in Table AIII.1. A general overview of all reactions that are operative has been reported in Chapter 2,[39] and the formation of oxidation products of methanol will be the focus Chapter5.[42]

4.2.2. General ligand effects in the reaction of nitrobenzene

The analysis of the reaction mixtures was carried out using gas–liquid chromatography (GLC); all products were quantified using calibration lines made from authentic samples. The accuracy of the quantitative analysis of the phenyl– containing products is excellent as confirmed by the sum of the aryl rings (column $\Sigma_\varnothing$ in Table 4.1, see also Table AIII.1). The conversions reached using the

palladium catalysts varies considerably with the ligand structure.[43] The conversion of nitrobenzene for all catalysts is moderate to high, ranging from 40 – 98%, corresponding to catalyst turnover numbers of 200–480.

Most catalysts containing a ligand with a propylene–backbone (entries 1, 3 – 5) are more selective towards carbonylation (~60%, column 'NCO') than towards hydrogenation (~40%, column 'NH'). For most catalysts containing a ligand with a butylene–backbone, this selectivity is reversed (~30% carbonylation and ~60% hydrogenation, entries 6, 8, and 9).

Table 4.1. Reactions of nitrobenzene with CO in methanol, catalyzed by a variety of Pd^{II}(ligand) complexes.[a]

Entry	Ligand	Conv. (%)[b]	Quantity (mmol)							Selectivity (%)[c]		
			PhNO$_2$	MPC	DPU	PhNH$_2$	Azo	Azoxy	$\Sigma_\varnothing$	NCO	N=N	NH
1	L3	67	8.1	5.9	1.7	5.1	0.1	0.4	23.5	49	6	44
2	L3X	67	8.1	5.3	0.8	8.3	0.1	0.4	24.3	38	6	56
3	oMeO–L3	53	11.5	6.6	0.9	4.1	0.1	0.1	24.4	58	3	39
4	oMeO–L3X	98	0.6	11.6	3.1	5.7	0.1	0.1	24.5	62	2	37
5	pMeO–L3	54	11.3	5.2	1.9	3.9	0.0	0.1	24.4	55	1	45
6	L4	60	9.8	3.0	0.8	5.4	0.2	2.1	24.4	26	32	42
7	L4X	52	11.8	0.5	0.5	1.9	0.1	4.5	24.4	8	73	19
8	oMeO–L4X	90	2.4	5.6	1.9	10.5	0.5	0.6	24.5	34	10	56
9	pMeO–L4	40	14.7	2.6	0.0	5.9	0.0	0.3	23.8	29	7	65

[a] Reactions were heated for four hours at 110 ºC in 25.0 ml dry and degassed methanol under 50 bar CO pressure. The catalyst was generated *in situ* from 0.05 mmol Pd(OAc)$_2$. Mole ratios are: Pd(OAc)$_2$: Ligand : nitrobenzene = 1 : 1.5 : 488. [b] Conversion = (24.4 –PhNO$_2$)/24.4 × 100%. [c] Selectivity towards carbonylation products = (MPC + DPU) / ($\Sigma_\varnothing$ – PhNO$_2$) × 100%; selectivity towards coupling products = (2×Azo + 2×Azoxy) / ($\Sigma_\varnothing$– PhNO$_2$) × 100%; Selectivity towards hydrogenation products = (PhNH$_2$ + DPU) / $\Sigma_\varnothing$ – PhNO$_2$ × 100%.

Interestingly, the selectivity towards Azo(xy) coupling products (column 'N=N') appears to depend strongly on the ligand bite–angle (β). catalysts containing unsubstituted ligands with a propylene backbone ($\beta \approx 90º$)[44, 45] yield approximately 6% coupling products (entries 1 and 2), whereas this is 32 – 73% (entries 6 and 7) when using similar ligands with a butylene backbone ($\beta \approx 94º$). The formation of coupling products can be suppressed in favour of the carbonylation reaction by equipping the aryl rings of ligands with electron–donating methoxy groups either in the *ortho* (10% coupling, entry 8) or *para* (7% coupling, entry 9) position, indicating that this effect is predominantly electronic

113

in origin. A similar, although less pronounced effect is observed for the ligands with a propylene backbone (entries 1 – 5). The effect of a larger ligand bite angle and the effect of methoxy substituents in aryl phosphane ligands appears to be a general phenomenon, as several ligands with larger bite angles gave similar results.

4.2.3. The effects of reactants and additives

4.2.3.1 Effect of the concentration of CO and PhNO₂

Several experiments were conducted in which the concentration of a specific reactant was varied. Shown in Figure 4.4 are the selectivities observed for the carbonylation (white bars), coupling (black bars) and the hydrogenation reactions (grey bars), when increasing the CO pressure from 25 to 100 bar (see Table AIII.1).
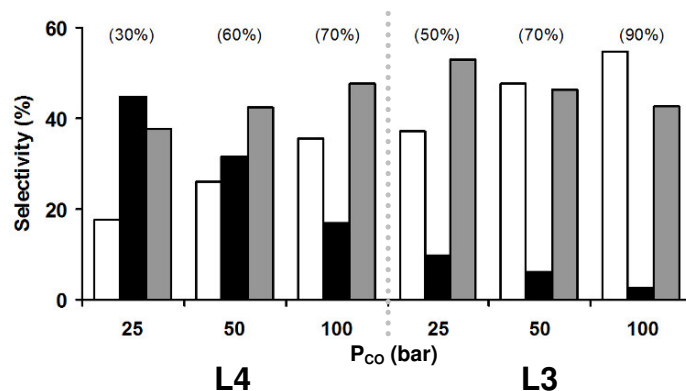
Figure 4.4. The selectivity of catalysts containing ligands L4 and L3 as a function of CO pressure (bar). Carbonylation products = □ = MPC + DPU; Coupling products = ■ = Azo + Azoxy; hydrogenation products = ■ = PhNH$_2$ + DPU. The conversion of nitrobenzene is given in parentheses.

Interestingly, for Pd^{II}(L4) as catalyst precursor, with increasing CO pressures the nitrobenzene conversion roughly doubles and the reaction becomes more selective towards both the carbonylation and hydrogenation products at the expense of the coupling products. When using Pd^{II}(L3) as catalyst precursor, the selectivity for

~ PhD Thesis: Towards a Sustainable Synthesis of Aromatic Isocyanates ~

carbonylation products increases at the expense of both the coupling and the hydrogenation products.

Because of a higher–than–unity molecularity in nitrobenzene for the formation of Azo(xy) coupling products, the initial concentration of nitrobenzene was also varied. The catalyst precursor $Pd^{II}(L4)$ was selected for investigation as for this catalytic system selectivity for coupling products is highest. As is shown in Figure 4.5 (see also Table AIII.1), the relative ratio of carbonylation (NCO) and hydrogenation (NH) products over coupling (N=N) products decreases significantly with increasing nitrobenzene concentrations, thus suggesting that the formation of Azo(xy) coupling products from nitrobenzene is competing with the carbonylation and hydrogenation reactions, but with higher order kinetics in nitrobenzene.
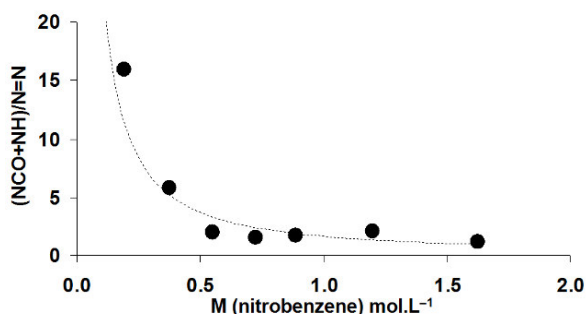
Figure 4.5. Plot of the ratio of (carbonylation (NCO) and hydrogenation (NH) products) relative to the amount of coupling products (N=N) as a function of the initial concentration of nitrobenzene in mol.l^{-1}, when using $Pd^{II}(L4)$ as catalyst precursor. The line is added as an aid for the eye.

4.2.3.2 Effect of the acidity of the reaction medium

As is shown in Table AIII.1 and Figure 4.6 for $Pd^{II}(L4X)$, upon addition of *para*–toluenesulfonic acid (HOTs) (pK_a = –2.7)[46] in sub–stoichiometric amounts on palladium the conversion of nitrobenzene increases from about 50% to a maximum of 84%, with a suppression of the coupling reaction (73 to 32%) in favor of the hydrogenation (15 to 49%) and carbonylation reactions (4 to 19%). When further increasing the acidity by adding an excess (4 eq.) of HOTs on palladium, the conversion decreases to 47%. At the same time however, the reaction becomes more selective towards hydrogenation (49 to 65%) and less selective towards coupling products (32 to 20%). The selectivity for carbonylation remains approximately constant.
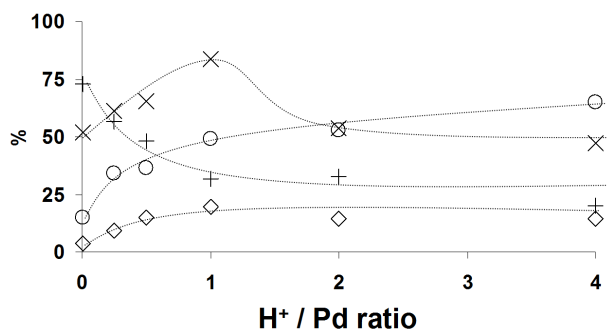
Figure 4.6. Plot of the conversion of nitrobenzene (×) and the selectivity towards coupling products (+, Azo(xy)), hydrogenation products (○, DPU + PhNH$_2$), and carbonylation products (◇, MPC + DPU) as a function of the amount of *p*–toluenesulfonic acid added (relative to Pd) when using the catalyst precursor Pd^{II}(L4X). The lines were added as an aid for the eye.

The addition of a base results in the reverse effect on conversion of nitrobenzene and selectivity for coupling products. The addition of only 2 eq. of a strong base ('Proton Sponge$^®$', i.e. 1,8–bis(dimethylamino)naphthalene (DMAN)) on palladium leads to a decrease of the conversion to 20%. Azo(xy) coupling products are formed almost exclusively (94%), while carbonylation is totally suppressed. The effects of addition of strong base and acid on selectivity and conversion of the catalyst based on L4X are depicted in Figure 4.7.
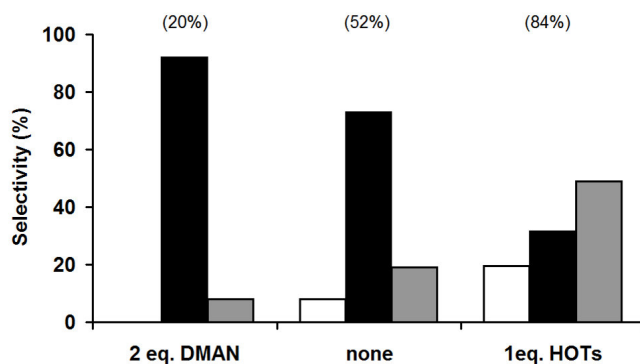
Figure 4.7. The selectivity when using Pd^{II}(L4X) and the indicated additive for: carbonylation products (□, MPC + DPU), coupling products (■, Azo + Azoxy), and hydrogenation products (■, PhNH$_2$ + DPU). The conversion of nitrobenzene is given in parentheses.

The effect of acidity on the system containing Pd^{II}(oMeO–L3X) as the catalyst precursor was also investigated, as this catalytic system is already very active in the absence of acid (96% conversion), while only producing ~2% coupling products. As can be seen in Figure 4.8, when adding up to four equivalents of

116

HOTs (on Pd), the conversion of nitrobenzene steadily decreases from 96 to 7%; at higher acid concentrations more hydrogenation products (40 to 70%) are produced at the expense of carbonylation products (60 to 30%).
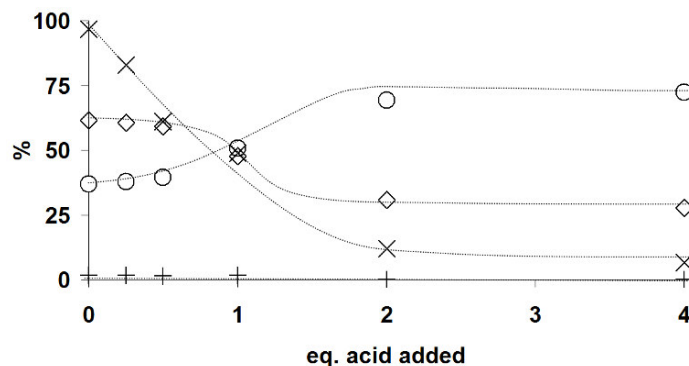
Figure 4.8. Plot of the conversion of nitrobenzene ($\times$) and the selectivity towards coupling products (+, Azo + Azoxy), hydrogenation products ($\bigcirc$, DPU + PhNH$_2$), and carbonylation products ($\diamond$, MPC + DPU) as a function of the amount of p–toluenesulfonic acid added (relative to Pd) when using the catalyst precursor Pd^{II}(oMeO–L3X). The lines are added as an aid for the eye.

Addition of a base 2 eq. of the base DMAN to the Pd^{II}(oMeO–L3X) catalytic system, results in a lower conversion of nitrobenzene, without a significant change in selectivity. The effects of addition of 2 equivalents of strong base or one equivalent of strong acid are compared in Figure 4.9, thus revealing that for this catalyst system the most significant effect is on conversion, which is lowered when adding either DMAN (from ~100 to 80%) or HOTs (from ~100 to 50%). The selectivity for coupling products remains very low in all instances.
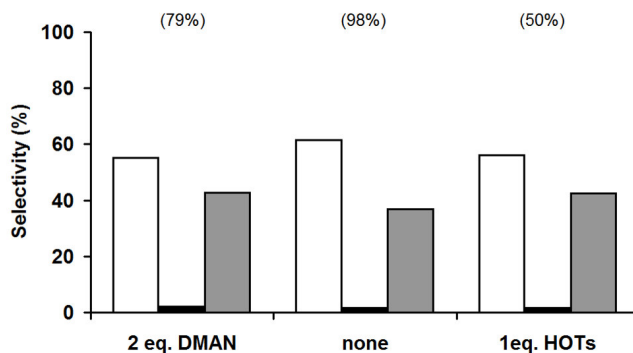
Figure 4.9. The selectivity when using oMeO–L3X and the indicated additive for: carbonylation products ($\square$, MPC + DPU), coupling products ($\blacksquare$, Azo + Azoxy), and hydrogenation products ($\blacksquare$, PhNH$_2$ + DPU). The conversion of nitrobenzene is given in parentheses.

To assess if the effect on the catalytic activity is dependent on the anion in the acid employed, reactions were performed adding half an equivalent of TMBA (trimethylbenzoic acid; pK_a = 3.43).[46] As is shown for the Pd^{II}(L4X) catalytic system in Figure 4.10a, irrespective of the acid, the same trend is observed: the conversion is increased while the formation of coupling products is suppressed in favor of carbonylation and hydrogenation products. This effect is more pronounced for the stronger acid HOTs compared to the weaker acid TMBA, suggesting that the effect really depends on the available concentration of protons. For the series with the Pd^{II}(oMeO–L3X) catalytic system (Figure 4.10b), the conversion decreases but the selectivity changes only slightly, irrespective of the acid. In both cases, when the reaction medium becomes more acidic, relatively more hydrogenation products are produced.
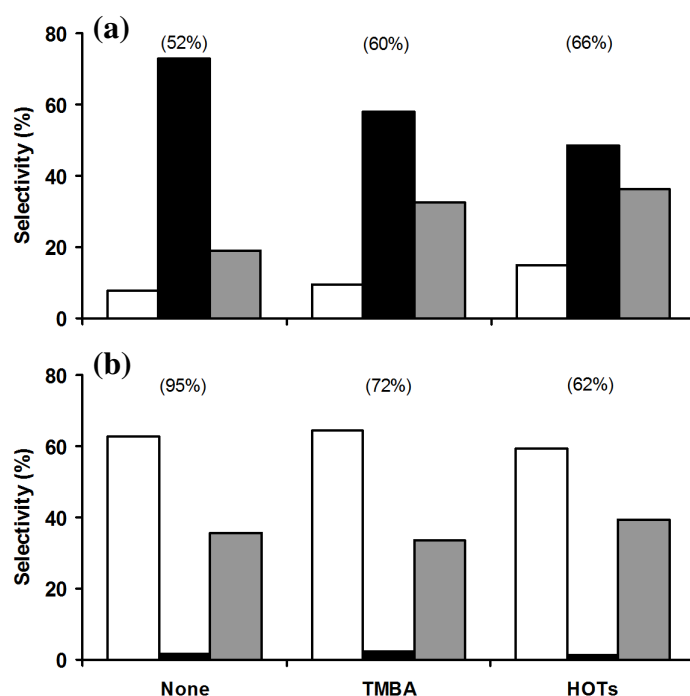
Figure 4.10. The product distribution in the carbonylation of nitrobenzene when using L4X (a) or oMeO–L3X (b), when adding 0.5 equivalent (on Pd) of the indicated acid. Carbonylation products = □ (MPC + DPU), coupling products = ■ (Azo + Azoxy) and hydrogenation products = ■, (PhNH$_2$ + DPU). The conversion of nitrobenzene is given in parentheses.

4.2.4. Investigations into the possible intermediacy of a pallada-cyclic complex

4.2.4.1 General considerations

The palladacyclic compound shown in Figure 2a, wherein L_2 = 1,10–phenanthroline (phen) has been characterized crystallographically. This complex can be synthesized under conditions very similar to those of catalytic experiments, and has been reported to be thermally stable to about 170 ºC.[16] Upon addition of an acid and heating to 90 °C in ethanol this complex decomposes to yield ethyl phenyl carbamate (80%).[16] The possible formation of such a palladacyclic compound in the diphosphane–based system was therefore investigated both experimentally and theoretically.

4.2.4.2 Attempted synthesis and DFT calculations

Attempts were undertaken to synthesize the diphosphane palladacyclic complexes with the ligands L3X and oMeO–L3X using the same procedure reported for the phen compound (ethanol, 60 °C).[16, 47] To verify whether a palladacyclic complex was formed at all, the reaction mixtures were analyzed with ^{31}P{^{1}H}–NMR analysis, directly after the presumed reaction took place. Only for the ligand L3X the analysis revealed the presence –besides various other products– of an un–symmetric complex (two doublets around 3.8 and 5.8 ppm, J = 30 Hz) that might well be the anticipated 'L3X–palladacycle'. However, all attempts to isolate this species from the complex mixture of products were unsuccessful, leading to reaction mixtures in which the un–symmetric complex disappeared in the course of experimentation. This led us to investigate the stability of such complexes theoretically, using DFT calculations. As the solid state structure of the 'phen–palladacycle' has been reported (i.e., (phen)PdC(O)ON(Ph)C(O) • PhNO$_2$),[47] this complex was calculated in order to validate the computational method (Figure 4.11a). The structural characteristics of the DFT–optimized structure are indeed very similar to those of the X–ray structure (Table 4.2). The minor variations might be due to crystal packing forces and the lattice nitrobenzene molecule.

Also given in Table 4.2 are selected characteristics of the palladacyclic complexes containing the ligands oMeO–L3X and L3X; perspective views of the calculated structures are given in Figure 4.11a1–c1. As expected, the P1–Pd–P2 coordination angle is about 90º for both phosphorus ligands, whereas the N1–Pd–N2 angle for

119

phen is 76º. Note that as the dihedral angle between the L1–Pd–L2 and C1–Pd–C2 planes increases along the series (from 0.86º for phen to 21.47º for L3X, see also Figure 11a2–c2), the L–Pd and C–Pd distances are elongated. With these geometric changes, the enthalpy of formation of the P_2–palladacycle –relative to the phen–palladacycle– decreases with 13.3 kcal.mol^{-1} for the L3X complex. This suggests that when the P–Pd–P angle is larger, the palladacyclic complex becomes more distorted and as a result becomes less stable, thus lowering the barrier for decomposition.

Table 4.2. Selected data of some (calculated) 'Ligand–palladacyclic' complexes (see also Figure 4.11).

| Complex (→): | X–ray | DFT (BP / 6–31G*) | | |
Parameter (↓):	phen	oMeO–phen	L3X	L3X
L1 – Pd (Å)	2.128	2.203	2.434	2.438
L2 – Pd (Å)	2.130	2.203	2.429	2.423
C1 – Pd (Å)	1.939	1.973	2.024	2.027
C1 – Pd (Å)	1.927	1.987	2.040	2.037
L1 – Pd – L2 (º)	77.66	76.04	90.98	90.68
C1 – Pd – C2 (º)	82.02	82.00	81.36	80.93
LLPd/PdCC (º)	1.89	0.86	16.30	21.47
'ΔH' (kcal.mol^{-1})[a]	–	–75.4	–65.3	–62.1
'ΔH'$_{rel}$ (kcal.mol^{-1})[b]	–	0	10.1	13.3

[a] The enthalpy of formation was calculated from: Pd(Ligand)(CO)$_2$ + PhNO$_2$ + CO → Complex + CO$_2$. [b] relative to 'phen–palladacycle'.
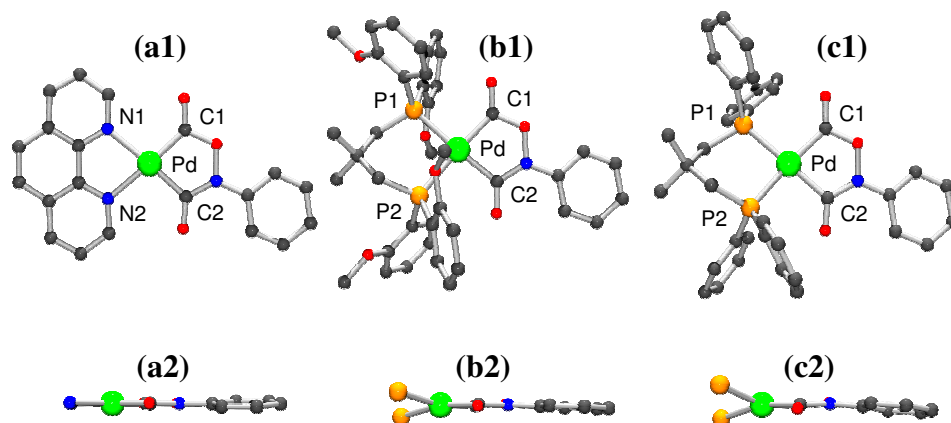
Figure 4.11. Perspective views of the calculated palladacyclic complexes with the ligands: (a1) phen (b1) oMeO–L3X; (c1) L3X. Side views for these complexes are shown in a2–c2, wherein only the donor–atoms of the ligands are shown for clarity. Color code: Pd (green), P (orange), N (blue), O (red), C (grey), H atoms are omitted for clarity.

~ PhD Thesis: Towards a Sustainable Synthesis of Aromatic Isocyanates ~

4.2.4.3 L3X–palladacycle synthesis via ligand exchange

As attempts to isolate P_2-palladacycle complexes were unsuccessful and DFT calculation indicate that these complexes are less stable than their phen analogue, it was subsequently considered to monitoring phenanthroline ligand exchange by L3X of the synthetically well–proven phen–palladacycle complex (Scheme 4.2)[16, 47] in the hope of learning more about the stability of such 'L3X–palladacycle' (**II**).
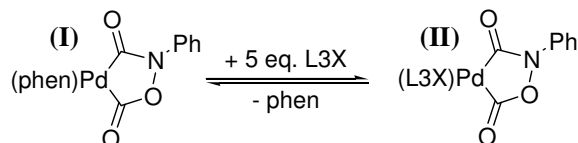
Scheme 4.2. Envisaged ligand exchange between 'phen–palladacycle' (**I**) and L3X to form 'L3X–palladacycle' (**II**).

An NMR experiment was conducted wherein (under an argon atmosphere) five equivalents of the free ligand L3X (dissolved in deuterated nitrobenzene) were added to one equivalent of the 'phen–palladacycle' (complex (**I**)). The yellow suspension was measured with $^{31}P\{^1H\}$–NMR, showing initially the resonance of ligand L3X around –25.1 ppm and only traces of a new complex around 4 – 6 ppm (Figure 4.12a), which was also observed in the reaction mixture of the attempt to synthesize (**II**) directly *via* nitrobenzene carbonylation.
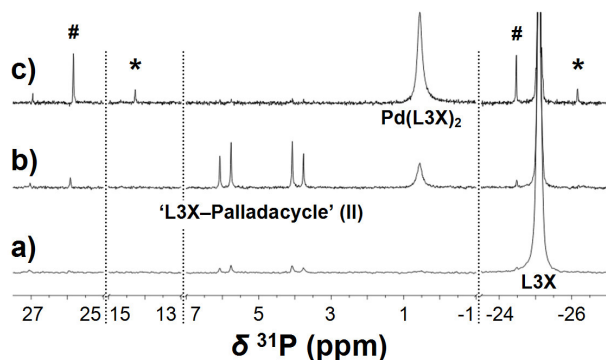
Figure 4.12. $^{31}P\{^1H\}$–NMR spectra for a solution containing 'phen–palladacycle' and 5 eq. of L3X in an argon atmosphere in nitrobenzene before heating (a), after heating to 60 °C for about one minute and then cooled to room temperature (b), after standing for an additional two hours at room temperature (c). # = the mono–oxide of L3X; * = the mono–phosphazene of L3X.

After gentle heating to about 60 °C for about one minute, a clear solution was obtained which was cooled to room temperature (~25 °C), and measured with

$^{31}P\{^{1}H\}$–NMR. As can be seen in Figure 4.12b, an un–symmetric diphosphane complex was formed, characterized by two doublets centred around 3.8 and 5.8 ppm (J = 30 Hz). In the ^{1}H–NMR spectrum of this solution, an isolated resonance is observed around 9.1 ppm, characteristic for uncoordinated phen, suggesting a successful ligand exchange. Assuming that L3X replaces phen as ligand while keeping the palladacycle intact, the $^{31}P\{^{1}H\}$–NMR spectrum could thus tentatively be assigned to the un–symmetric 'L3X–palladacyle' complex (**II**).

The un–symmetric complex is unstable and disappears in about two hours at room temperature, while a new broad resonance around 0.5 ppm appears. This resonance belongs to the neutral bis–ligand complex [$Pd^{0}(L3X)_2$], as verified by *in situ* synthesis of [$Pd^{0}(L3X)_2$] from [$Pd_2(dba)_3$] (dba = dibenzylidene acetone) and 10 equivalents of L3X in nitrobenzene (Figure AIII.1). After the *in situ* synthesis of [$Pd^{0}(L3X)_2$], resonances due to some mono–oxidized ligand ('P=O'; 25.8 and –24.5 ppm) and some di–oxidized ligand ('O=PP=O'; 27.0 ppm) are present as well (Figure AIII.1). These same resonances are also found in the ligand exchange experiment (Figure 4.12), but two additional resonances are observed around 14.3 and –26.2 ppm (marked with '*' in Figure 4.12c). These resonances grow equally fast, indicating that they belong to the same species. Obviously, this species is not ligand mono–oxide, nor can this be a divalent palladium complex; [$Pd^{II}(L3X)(OAc)_2$] is characterized by a sharp singlet around 16 ppm and [$Pd^{II}(L3X)_2$]($OTs)_2$ exhibits a broad resonance around 5 ppm.[40] This leaves as the only likely option the formation of a phosphazane ('P=NPh'), which must be formed during the decomposition of the initially formed un–symmetric 'L3X–palladacycle' complex (**II**). The presence of such a phosphazene was also observed with Electron Spray Ionization Mass Spectroscopy (*vide infra*).

To further characterize the decomposition pathway of the postulated 'L3X–palladacycle'complex (**II**), the ligand exchange experiment was repeated under an atmosphere of carbon monoxide. The kinetic data of this experiment are shown in Figure 4.13b, while Figure 4.13a shows the kinetic data for the reaction under argon. The rate of appearance of [$Pd^{0}(L3X)_2$] (0.5 ppm, 0.0021 and 0.0004 min^{-1}) is about twice the rate of the disappearing $^{31}P\{^{1}H\}$–NMR signals at 3.8 and 5.8 ppm (–0.0011 and –0.0002 min^{-1}), which is consistent with the assignment of the disappearing compound to a compound containing one diphosphane ligand (two P–atoms, possibly 'L3X–palladacycle' (**II**)), and the appearing species to

~ PhD Thesis: Towards a Sustainable Synthesis of Aromatic Isocyanates ~

[Pd⁰(L3X)₂] (four P–atoms). The decomposition of the presumed 'L3X–palladacycle' (**II**) is approximately five times slower for the reaction under carbon monoxide atmosphere (–0.0002 min⁻¹) compared the reaction in argon (–0.0011 min⁻¹). In a CO atmosphere less [Pd⁰(L3X)₂] is formed during the initial ligand exchange reaction (the intercept is 0.046 (CO) *versus* 0.074 (Ar)).
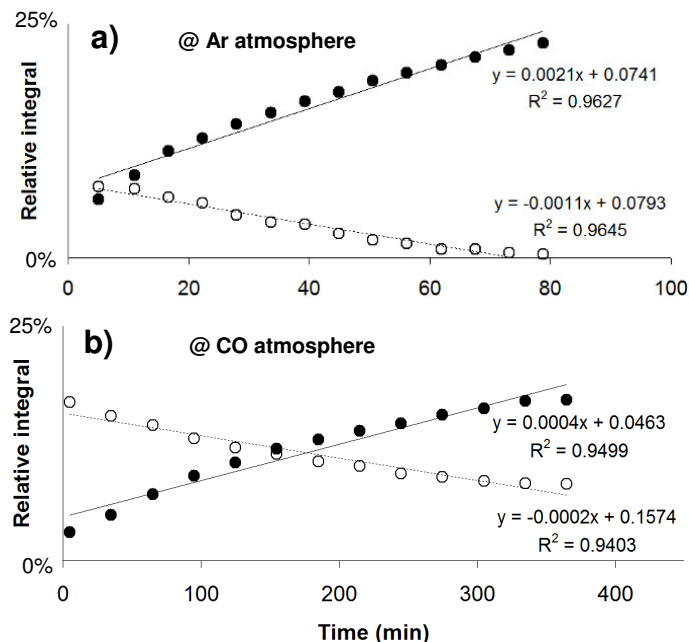
Figure 4.13. Plot of the ³¹P{¹H}–NMR integrals (relative to the ligand and the appearing and disappearing compounds) for the resonance of [Pd⁰(L3X)₂] around 0.5 ppm (●) and 'L3X–palladacycle' around 5 ppm (○) as a function of time; a) under an argon atmosphere; b) under an atmosphere of CO.

4.2.4.4 Ligand exchange experiment with 1 eq. L3X and ESI–MS analysis

The above data strongly suggest that the 'L3X–palladacycle' complex (**II**) formed from Phen–L3X exchange is unstable and decomposes at ambient temperatures (~25 °C); the stabilizing effect of a CO atmosphere indicates that this proceeds *via* a reversible decarbonylation / carbonylation process. Apparently, extrusion of CO_2 from the 'L3X– palladacycle' (**II**) has a higher barrier than decarbonylation, as also judged from the fact that only traces of isocyanate are formed (*vide infra*). In an attempt to prevent the decomposition of 'L3X–palladacycle'(**II**) to [Pd⁰(L3X)₂], which possibly is accelerated by the presence of excess of L3X, and

in order to detect possible intermediate species in the presumed decarbonylation of 'L3X–palladacycle' (**II**), the ligand exchange experiment was repeated with only one equivalent of L3X. The resulting spectra are shown in Figure 4.14.
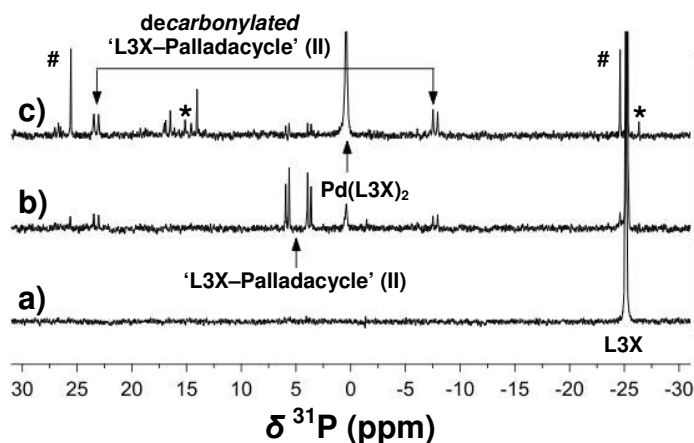
Figure 4.14. ^{31}P{^{1}H}–NMR spectra for a solution containing 'phen–palladacycle' and 1 eq. of L3X in nitrobenzene before heating (a), after heating to 60 ºC for about one minute and cooling to room temperature (b), after standing for an additional 180 minutes at room temperature (c). # = the mono–oxide of L3X; * = the mono–phosphazene of L3X.

The ^{31}P{^{1}H}–NMR spectrum of the yellow suspension obtained after mixing 'phen–palladacycle'(**I**) with one equivalent of L3X in nitrobenzene initially shows only pure ligand (–25 ppm, Figure 4.14a). The reaction mixture was then heated gently to about 60 °C for about one minute, and after cooling to room temperature the resulting clear orange solution was again measured with ^{31}P{^{1}H}– NMR (Figure 4.14b). Besides the resonances of the anticipated un–symmetric species around 5.0 ppm and some [Pd^0(L3X)$_2$] around 0.5 ppm, two additional weak doublet signals were observed around 23.9 and –7.1 ppm which evolved at the same rate and have an identical coupling constant (J = 42 Hz). This is consistent with the formation of another un–symmetric mono–chelate palladium complex, which may well be a de*carbonylated* 4–membered ring 'L3X– palladacycle' complex (**III**) with the proposed structure shown in Scheme 4.3 (see also next section). The formation of another decarbonylated 4–membered ring L3X–palladacycle complex (**IV**) was also considered (Scheme 4.3). However, the large difference in chemical shift (31 ppm) between the two phosphorus nuclei is

more consistent with palladacycle (**III**), as the Pd–C(O)O–moiety will cause severe deshielding (23.9 ppm), while the Pd–N(Ph)– moiety will cause significant shielding (–7.1 ppm). The weak resonances observed between 14–18 ppm may then perhaps arise from the 4–membered L3X–palladacycle complex (**IV**).
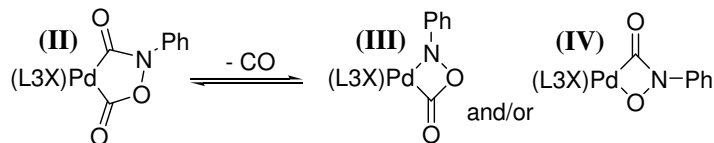
Scheme 4.3. Proposed structure of 4–membered ring 'L3X–palladacycle' complexes (**III**) and (**IV**) formed after decarbonylation of 5–membered ring 'L3X–palladacycle' complex (**II**).

After the solution was allowed to stand at room temperature for an additional 180 minutes (Figure 4.14c), the 'L3X–palladacycle' (**II**) is almost absent, while the (presumed) decarbonylated 4–membered 'L3X–palladacycle'(**III**) is still significantly present (~20% based on Pd;[48] see also Figure AIII.2). [Pd⁰(L3X)₂] has become the major species (33% based on Pd). Amongst the several unknown species that have evolved (resonances between 14 and 18 ppm; 25% based on Pd) the presence of L3X–palladacycle complex (**IV**) can neither be proven nor be ruled out. Some ligand mono–oxide is formed ('P=O'; 25.8 and –24.5 ppm), and some uncoordinated ligand (–25.1 ppm) is still present, thus suggesting that the ligand exchange reaction is not quantitative after 180 minutes; this is corroborated by ¹H–NMR showing that 'phen–palladacycle' (**I**) is also still present in approximately the same amount as uncoordinated L3X.[48]

These results strongly suggest the initial formation of 'L3X–palladacycle' (**II**) on ligand exchange of L3X with phen–palladacycle (**I**), while its subsequent disappearance seems to proceed *via* a decarbonylation process to give either 4–membered L3X–palladacycle complex (**III**) or (**IV**), or both. To obtain more evidence for the decarbonylation pathway, the ligand exchange experiment was repeated and after gentle heating the clear solution was now measured with electron spray ionization mass spectroscopy (ESI–MS). In the resulting mass spectrum (Figure 4.15), the highest observed mass (*m/z* 986.2) originates from [Pd(L3X)₂]⁺ (exact mass = 986.3).
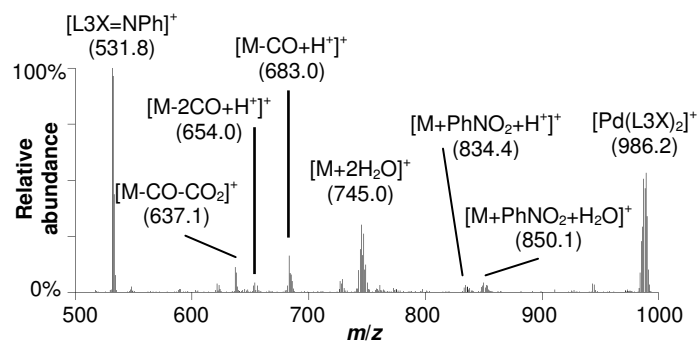
Figure 4.15. ESI mass spectrum of reaction mixture taken directly after the ligand exchange of phen-palladacycle (**I**) with one equivalent of L3X. M = 'L3X–palladacycle' (**II**) = [(L3X)PdC(O)ON(Ph)C(O)].

As the lower mass products observed are absent in an ESI–MS of pure [Pd^0(L3X)$_2$] in nitrobenzene, these lower mass peaks must originate from other complexes formed in the exchange reaction. Although the exact mass (709.1) of the presumed 'L3X–palladacycle' (**II**) is not observed, various peaks and their isotope distributions are consistent with solvent adducts of 'L3X–palladacycle' (**II**), as is detailed in Figure 4.16.
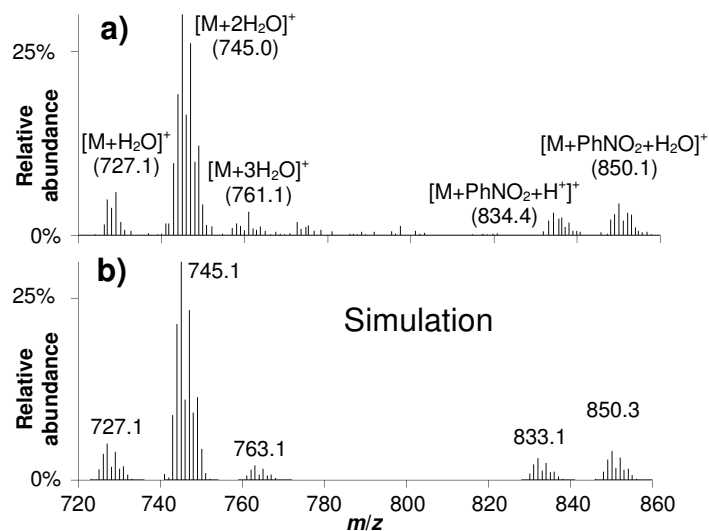
Figure 4.16. (a) Zoom–in and assignment of the ESI mass spectrum of reaction mixture from *in situ* synthesis of 'L3X–palladacycle' (**II**) (=M); (b) simulation.

In the ESI–MS of the reaction mixture (Figure 4.15) a small peak is present with a mass corresponding to the decarbonylated 'L3X–palladacycle' (**III**) or (**IV**) ([M–CO+H$^+$]$^+$; 683.0), whereas the mass of decarboxylated 'L3X–palladacycle' ([M–CO$_2$]$^+$; exact mass = 665.1) is not observed. The small peak at m/z 654.0 corresponds to [M–2CO+H]$^+$, i.e. nitrosobenzene bound to [(L3X)Pd^0]. Interestingly, the small feature at m/z 637.1 can be assigned to [M–CO–CO$_2$]$^+$, which corresponds to an imido complex '(L3X)Pd=NPh' (**V**). The presence of a (L3X)Pd(ONPh) and a (L3X)Pd=NPh (**V**) complex as fragmentation products of 'L3X–palladacycle' (**II**), is very likely reflecting its thermal decomposition pathway. The reaction product of (L3X)Pd=NPh with L3X (i.e. the phosphazene '[L3X=NPh]$^+$'; m/z 531.8) is clearly present as well (see also ^{31}P{^{1}H}–NMR above), while small quantities of aniline and nitrosobenzene are observed with GLC–MS.

These MS data are thus in agreement with the NMR data, and suggest that the initially formed 5–membered P$_2$–palladacycle may (at least partially) decompose to a P$_2$Pd–imido species, *via* (**III**), as is shown in Scheme 4.4. The imido complex (**V**) may then, at least partially, reacts with coordinated P$_2$ ligand to the observed phosphazene while liberating zero–valent palladium, which is trapped by uncoordinated L3X as [Pd^0(L3X)$_2$].
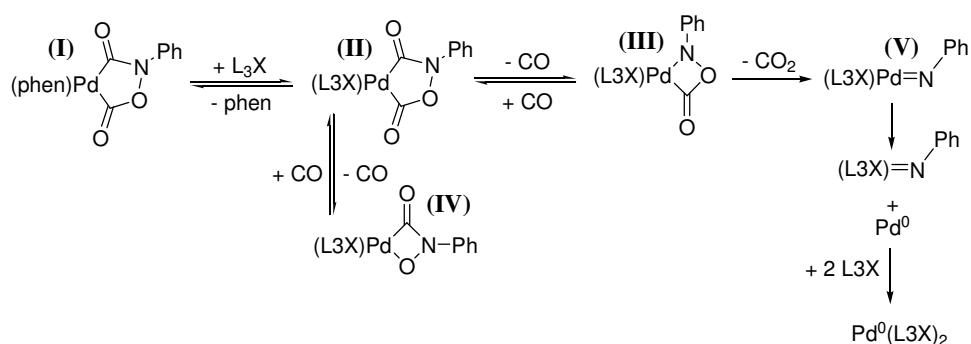
Scheme 4.4. Proposed reaction sequence of the ligand exchange between 'phen–palladacycle' (**I**) and the diphosphane ligand L3X, followed by decomposition of the 'L3X–palladacycle' (**II**).

4.2.4.5 Attempted identification and quantification of 'PhN'–containing products

The reaction sequence shown in Scheme 4.4 cannot be the entire story however, as the formation of 'L3X=NPh' is by no means quantitative with respect to the amount of 'PhN' that was initially present in the form of phen–palladacycle (**I**) (~10 μmol). The integrals of 'L3X=NPh' and [Pd^0(L3X)$_2$] by the end of the ligand exchange experiment (Figure 4.14c) indicate that merely ~0.4 μmol of the initial 'PhN' ends up in the L3X–phosphazene.[49] Likely products that may contain the remaining ~9.6 μmol of the 'PhN' fragment could be aniline, phenylisocyanate, nitrosobenzene and/or azo(xy)benzene. Because the ^{1}H–NMR resonances of all possible reaction products containing the 'PhN' moiety are obscured by the resonances of the abundantly present nitrobenzene, L3X, and [Pd^0(L3X)$_2$], the solution was analyzed with GLC–MS. However, using this technique it only proved possible to positively identify about 10% of the NPh fragment originally present in complex (**I**) as aniline, nitrosobenzene, phenyl isocyanate and L3X=NPh.

To obtain more unambiguous information about the fate of the 'PhN' moiety the NMR experiment was repeated in non–aromatic solvents such as CH$_3$NO$_2$ and CD$_2$Cl$_2$ (see Appendix III, section AIII.3.1) Although these experiments strongly suggest the formation of *various* 'PhN' containing products, neither a positive identification nor quantification could be achieved, mostly due to the interference of the aromatic resonances of L3X and Pd^0(L3X)$_2$. Experiments using a ligand with pentafluorophenyl groups were also inconclusive, but again showed the formation of various 'PhN'–containing products (see Appendix III, section AIII.3.2).

4.2.4.6 Ligand exchange experiment with a bulky phosphane ligand

In an attempt to stabilize a possible 'Pd=NPh' species, the ligand exchange experiment was repeated with 5 equivalents of the sterically very bulky[50] phosphane ligand 1,3–bis(1,3,5,7–tetramethyl–4,6,8–trioxa–2–phospha-amantane)propane (bpap, Figure 4.17). Unfortunately, the anticipated ligand exchange reaction was not observed when the yellow 'phen–palladacycle' (**I**) / bpap suspension in nitrobenzene was carefully heated; only the resonances of the free ligand were observed around –31.0 (*rac*) and –30.2 (*meso*) ppm.[51] When the

solution was heated for four hours at 100 °C, small peaks of various unidentified

species evolved between 0 and 15 ppm (see Figure AIII.3 for $^{31}P\{^1H\}$–NMR spectrum). Most resonances lie around +28 and –30 ppm ('free' bpap), which most likely belong to ligand oxide or possibly also phosphane species such as 'bpap=NPh' or 'bpap(=NPh)$_2$'.
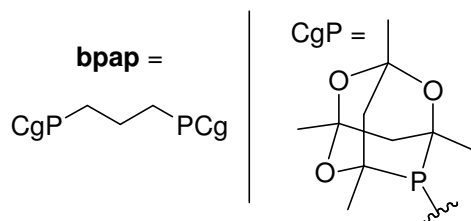
bpap =

Figure 4.17. Drawing of 1,3–bis(1,3,5,7–Tetramethyl–4,6,8–trioxa–2–phosphaamantane)-propane (bpap), used as mixture of the *rac* (*αα/ββ*) and *meso* (*α/β*) diastereoisomers (1:0.3 ratio).

To investigate whether a 'Pd=NPh' species is present amongst the species observed by NMR, the reaction mixture was analyzed with ESI–MS spectroscopy; the resulting mass spectrum is shown in Figure 4.18. The largest peak around m/z = 687 and its isotope distribution (see inset figure) are in perfect agreement with [(bpap)Pd=NPh·H$_2$O]$^+$ (which may also be written as [(bpap)Pd(OH)NHPh]$^+$). The second largest peak with mass around m/z 564 is consistent with the mono phosphazane of bpap, [bpap=NPh+H]$^+$ (exact mass of 564.3). The highest observed masses around m/z = 1051 and 1069 are relatively small and are consistent with [Pd(bpap)$_2$+H]$^+$ and [Pd(bpap)$_2$+H$_2$O+H]$^+$ (exact masses 1051.3 and 1069.3 respectively). These data thus again point to the palladium-imido complex as intermediate decomposition product of (**I**) via a ligand exchange as was shown in Figure 4.14.
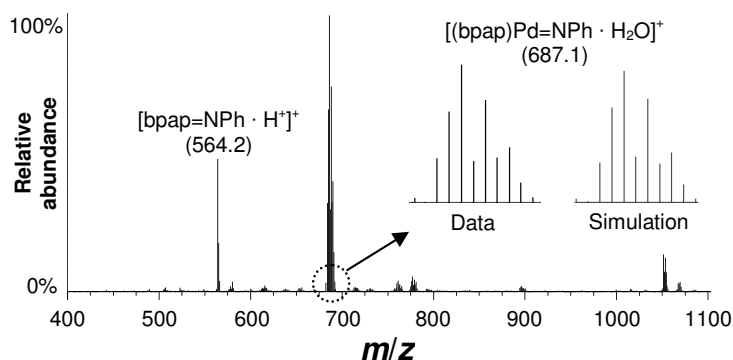
Figure 4.18. ESI mass spectrum of a solution containing 'phen–palladacycle'(**I**) and 5 eq. of bpap in nitrobenzene, after heating four hours at 100 °C. Inset: an enlargement of the indicated area, with a simulation of that mass.

129

These data are thus in agreement with the data obtained from ligand exchange and ESI-MS experiments with L3X in that an initially formed 5–membered P$_2$–palladacycle may (at least partially) decompose to a P$_2$Pd–imido species, *via* (**III**), as is shown in Figure 4.14. The imido complex (**V**) then, at least partially, reacts with coordinated P$_2$ ligand to the observed phosphazene while liberating zero–valent palladium, which is trapped by uncoordinated L3X as [Pd^0(L3X)$_2$].

4.2.5. Investigations into the possible existence of di-phosphane palladium imido complexes

4.2.5.1 DFT calculations

As the above all points towards a palladium–imido intermediate as a species of crucial importance, DFT calculations were performed to gain insight into the geometric and electronic properties of diphosphane–palladium–imido complexes. As a means of validating the computation method, the structure of the reported Ni–imido compound 1,2–*bis*–(di–tert–butylphosphanyl)ethane)Ni=N(Mes)[38] was calculated (Figure 4.19a). As can be seen in Table 4.3, characteristic distances and angles for the DFT–optimized structure are almost identical to those of the crystal structure of the nickel–imido compound. The only noticeable difference is the Ni–N–C angle, which is 180º in the crystal structure and 178.7º in the calculated structure.

Table 4.3. Selected data of several (calculated) imido complexes.

Complex (→):	Ni – Imido[a]		Pd – imido[b]		
Parameter (↓):	X–ray[38]	DFT	L4	pMeO–L4	L3X
Distances (Å)					
M=N	1.703	1.707	1.885	1.888	1.878
M–L1	2.189	2.195	2.279	2.323	2.274
M–L2	2.181	2.183	2.323	2.279	2.322
Angles (º)					
P1 – M – P2	90.94	90.95	97.56	97.27	92.48
P1 – M – N	134.4	134.6	146.7	146.0	151.7
P2 – M – N	134.4	134.4	116.6	116.7	115.6
Q(N)$_{NPA}$			−0.817	−0.848	−0.833
pK$_a$[c]			11.2	16.6	13.9
Azoxy selectivity	–	–	32%	7%	6%

[a] 1,2–*bis*–(di–tert–butylphosphanyl)ethane)Ni=N(mesityl).[38] [b] (ligand)Pd=NPh. [c] pK$_a$ = (Q(N)$_{NPA}$ * −174) −131 (R^2 = 0.983)[52]

~ PhD Thesis: Towards a Sustainable Synthesis of Aromatic Isocyanates ~

Considering the computational method valid, several P_2Pd^{II}=NPh complexes were calculated. As the catalyst system based on Pd^{II}(L4) produces significant amounts of azoxybenzene, and because azoxybenzene production can be suppressed by equipping the ligand aryl rings with electron–donating methoxy groups or by decreasing the bite angle, the series of Pd–imido complexes (L4)Pd^{II}=NPh, (pMeO–L4)Pd^{II}=NPh, and (L3X)Pd^{II}=NPh has been calculated. Characteristic data are listed in Table 4.3, and perspective views of the calculated structures are shown in Figure 4.19b–d.

Figure 4.19. Perspective views of the calculated imido complexes: (a) 1,2–*bis*–(di–tert–butyl-phosphanyl)ethane)Ni=N(2,4,6–trimethylphenyl); (b) (L4)Pd^{II}=NPh; (c) (pMeO–L4)Pd^{II}=NPh; and (d) (L3X)Pd^{II}=NPh. Color code: Ni (pink), Pd (green), P (orange), N (blue), O (red), C (grey), H atoms are omitted for clarity.
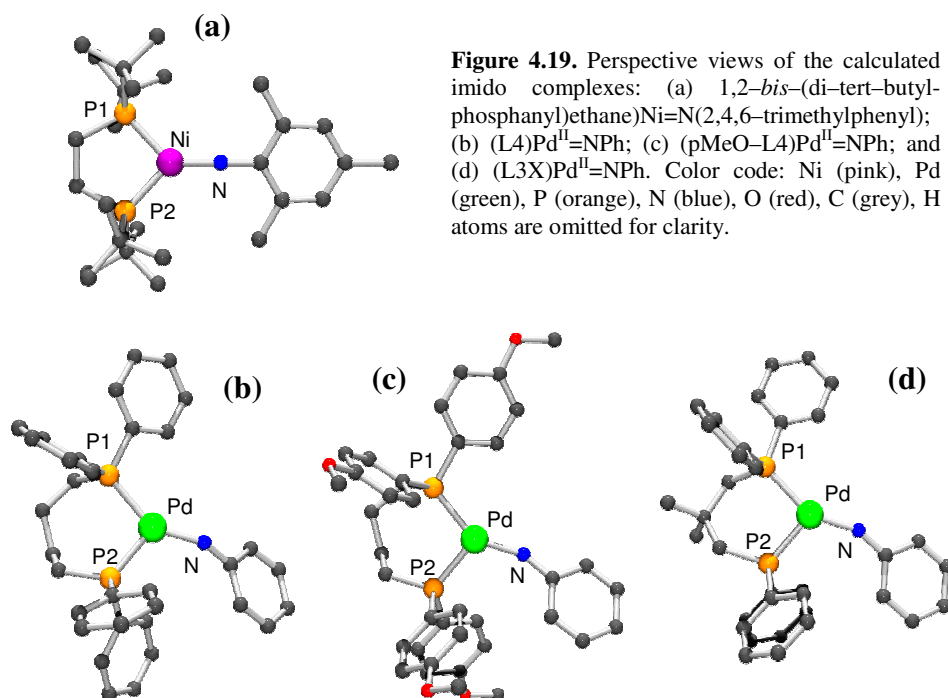
As expected, the main geometric difference between these computed complexes is the P1–Pd–P2 angle, which is larger (97º) for the complexes bearing a ligand with a butylene backbone compared to the propylene–bridged analogue (92º). The angle P1–Pd=N is about 152º when using L4 and pMeO–L4, compared to 146º when using L3X, showing that these complexes are asymmetric, in contrast to the

Ni–imido complex (both P–Ni=N angles are 135º). This geometric difference between these Ni– and Pd– imido complexes is probably due to the bulkier phosphane ligand used in the nickel compound (i.e., forcing the symmetry). A practical consequence of this is that the equatorial position *cis* to P1 in the $P_2Pd=NPh$ complexes is fairly open for incoming substrates.

When comparing the charge density on the imido–nitrogen atom based on the natural population analysis $(Q(N)_{NPA})$,[53] it appears that its basicity is smallest $(Q(N)_{NPA} = -0.817, pK_a = 11.2)$[52] in $(L4)Pd^{II}=NPh$, which, from this series of catalyst precursors, is the most selective towards Azoxy formation (32%).[54] For the other two complexes, which are far less selective towards Azoxy, the $Q(N)_{NPA}$ and the related pK_a are larger.

4.2.5.2 Synthesis of a palladium–imido complex and its reactivity with CO/CH₃OH

Attempts were undertaken to synthesize a $P_2Pd^{II}=NR$ complex and study its reactivity towards CO/CH₃OH. To the best of my knowledge, the synthesis of Pd– imidoaryl complexes has not been reported so far. Only in one instance has the detection of a particular class of group 10 metal (fluoro–alkyl) imido complexes been claimed, based solely on IR–spectroscopic measurements.[55] The synthesis of $P_2Ni^{2+}=NR$ complexes has been reported, however.[36-38] These reports were therefore chosen as the starting point for synthetic investigations. Thus, the reaction of a $P_2Pd^0(dba)$ complex with an aryl azide was envisaged to yield the corresponding imido complex with the extrusion of dinitrogen (Scheme 4.5). In order to protect and stabilize the supposedly reactive Pd=N–R bond the sterically crowded diphosphane ligand bpab and mesitylene (Mes) azide were used in this attempt.
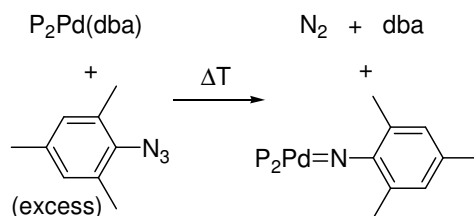
Scheme 4.5. Reaction scheme for the synthesis of a Pd–imido complex.

Selected ^{31}P{^{1}H}–NMR spectra of reaction mixtures for the *in situ* formation of [(bpap)Pd^{II}=NMes] are shown in Figure 4.20. The ^{31}P{^{1}H}–NMR spectrum of the starting compound [Pd^{0}(bpap)(dba)] in d^{8}–toluene shows two broad resonances around 2.5 and 5.0 ppm, due to the presence of *rac* (*αα/ββ*) and *meso* (*α/β*) diastereoisomers of bpap (Figure 4.20a).[51, 56] The small resonances around 28 and 29 ppm are due to the presence of a small amount of ligand oxide ('P=O'). No changes in the NMR are observed when an excess of mesitylene azide is added, not even after heating to 50 °C (not shown). The reaction mixture was therefore heated to 100 °C for about 30 minutes (Figure 4.20b) after which the reaction mixture was allowed to cool to room temperature (Figure 4.20c).
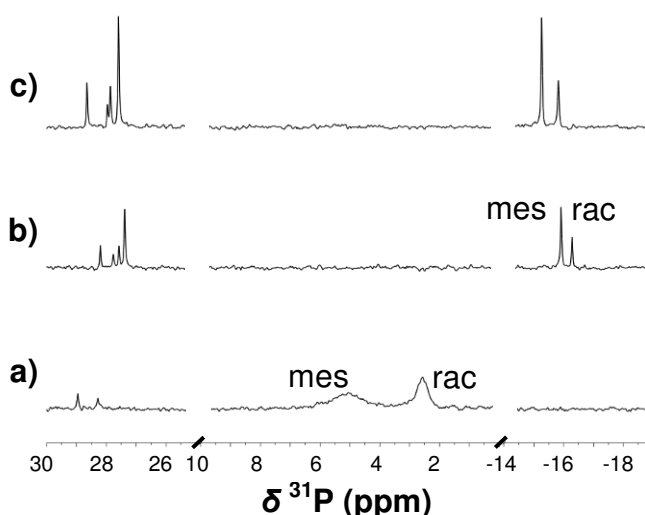
Figure 4.20. ^{31}P{^{1}H}–NMR spectra of reaction mixtures for the *in situ* formation of of [(bpap)Pd=NMes] in d^{8}–toluene, from [Pd(bpap)(dba)] and mesitylene azide: (a) pure [Pd(bpap)(dba)]; (b) after mesitylene azide addition and heated at 100 °C; (c) after cooling to room temperature.

After heating to 100 °C all [Pd^{0}(bpap)(dba)] has reacted as is evidenced by the disappearance of the resonances around 2.5 and 5.0 ppm. The resonances that were assigned to ligand oxide ('P=O', 28.0 and 28.7 ppm) have grown somewhat and two new resonances appeared around 27.6 and 27.9 ppm, which are assigned to a phosphazene moiety ('P=NMes', also observed with mass spectroscopy, *vide infra*). In addition, two resonances are observed around –15.3 and –15.8 ppm.

133

These resonances cannot be due to uncoordinated mono–oxide or mono–phosphazene version of the ligand, as the ^{31}P{^{1}H}–NMR resonances of the free ligand moiety are positioned around –31.0 (*rac*) and –30.2 (*meso*) ppm.[51] The resonances around –15.3 and –15.8 ppm may be assigned to the anticipated palladium–imido species [(bpap)Pd^{II}=NMes].[57] The DFT–calculations of such imido–complexes with phosphane ligands L4, L4X, and L3X (*vide infra*) suggest that these complexes are slightly asymmetric, and should thus appear as a double doublet in ^{31}P{^{1}H}–NMR. The singularity of the observed resonances around –15.3 and –15.8 ppm may well be explained by a thermal equilibrium process, but also by the very bulky ligands surrounding Pd, hence forcing higher symmetry as is observed for similar P_2Ni^{2+}=NR complexes with bulky P_2 and NR ligands.[36-38]

The reaction mixture was diluted with CH$_3$CN and analyzed with ESI–MS; part of the resulting mass spectrum is shown in Figure 4.21a, while Figure 4.21b shows a simulation of the three most prominent features in the spectrum.
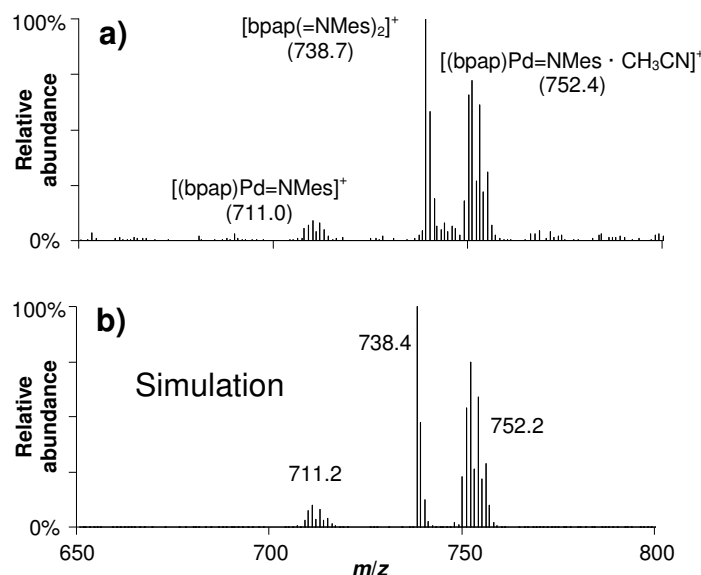
Figure 4.21. (a) ESI mass spectrum of diluted (CH$_3$CN) reaction mixture from *in situ* synthesis of [(bpap)Pd=NMes] from the NMR study; (b) simulation of the three most prominent MS peaks.

The highest mass (*m/z* 752.4) and its isotope distribution is in excellent agreement with a species [(bpap)Pd=NMes · CH$_3$CN]$^+$. The mass and isotope distribution at

~ PhD Thesis: Towards a Sustainable Synthesis of Aromatic Isocyanates ~

m/z = 711.0 may be assigned to [(bpap)Pd^{II}=NMes]$^+$ (calc. = 711.2). The mass centred on m/z = 738.7 is assigned to the double phosphazane ('MesN=PP=NMes'; calc. = 738.4). Also present but not shown in the figure is a small peak belonging to bpap containing one phosphorus oxide and one phosphazane ('O=PP=NMes', m/z = 621.3). It is noteworthy that mono–phosphazene–phosphane ligand is not observed, consistent with the ^{31}P{^{1}H}NMR spectra shown in Figure 19. The formation of the observed diphosphazane compounds may result from the Staudinger reaction of the azide with possibly uncoordinated phosphane ligand.[58] The formation of the diphosphazane could also imply however, that [(bpap)Pd^{II}=NMes] acts as the imidation agent for the diphosphane ligand. The NMR and ESI–MS results are both consistent with the formation of [(bpap)Pd^{II}=NMes] as shown in Scheme 4.5.

Finally, a new reaction mixture of (bpap)Pd^{II}=NMes was prepared as described above, whereafter CO was bubbled though the solution for about five minutes at 25 °C followed by the addition of CH$_3$OH. The addition of methanol may trap any possibly formed mesitylene isocyanate, or react with solvated CO and the imido complex to yield methyl mesityl carbamate. The resulting reaction mixture was analyzed with GLC–MS, clearly revealing the presence of methyl mesityl carbamate with a retention time t_R of 20.8 minutes (~20% peak intensity, indicating that it is formed from the metal–imido intermediate),[59] and an m/z of 193 (exact mass = 193.1; Figure AIII.11). The unlikely event[60] that methyl mesityl carbamate is formed by direct reaction between the excess of mesityl azide, CO and methanol –without involvement of the palladium complex– was also considered. However, when methanol is added to a CO saturated solution of mesityl azide, and the resulting solution is analyzed with GLC–FID, methyl mesityl carbamate is not observed.

It is thus concluded, both from spectroscopic evidence as well as from the observed reactivity of the complex with CO/Methanol, that a species has been synthesized that appears to be a first 'Pd=NAr' complex. It also demonstrates that such Pd=NPh species can be methoxy-carbonylated to produce carbamate (and a zero-valent Pd species) under mild conditions.

4.3. Discussion

4.3.1. A complex network of catalytic reactions centred around a P_2Pd^{II}=NPh complex

As explained in detail in Chapter 3, a remarkable observation when applying bidentate diarylphosphanes as ligands in the palladium catalyzed carbonylation of nitrobenzene is the formation of substantial amounts of methanol oxidation products such as DMC, DMO, MF, and CO.[39] During the formation of these products, H–atoms are liberated, which are transferred to nitrobenzene and are observed in the products $PhNH_2$, DPU and H_2O. Thus, apart from CO, methanol functions as a reductant and hydrogen transfer reagent for nitrobenzene. This provides very important mechanistic information; the oxidation of methanol is clearly coupled with the reduction of nitrobenzene involving Pd^0/Pd^{II} chemistry.

To sustain catalytic cycles for both the methanol oxidation products as well as for the nitrobenzene reduction products, a product–releasing species of the one cycle must be an initiating intermediate in the complementary product cycle. In Chapter 3 it was proposed that a Pd–imido species, (P_2Pd^{II}=NPh) is such a key intermediate to several product–generating catalytic cycles, as is briefly summarized below.[39]

Nitrobenzene reduction to the imido–complex involves oxidation of Pd^0 to Pd^{II}, and can be described by the three half–reactions given in Equations 1a–c. The nitrobenzene deoxygenating reagents are respectively two molecules of CO (1a), one CO and two acidic CH_3OH H–atoms (1b), or all H–atoms from one CH_3OH molecule (1c). The formation of DMO can be seen as a modified version of Equation 1b (with 2 CO), and the formation of MF can be regarded as a modified version of Equation 1c (with 2 CH_3OH).

$$P_2Pd^0 + PhNO_2 + 2\ CO \rightarrow P_2Pd^{II}\text{=NPh} + 2\ CO_2 \tag{1a}$$
$$P_2Pd^0 + PhNO_2 + 2\ CO + 2\ CH_3OH \rightarrow P_2Pd^{II}\text{=NPh} + H_2O + CO_2 + DMC \tag{1b}$$
$$P_2Pd^0 + PhNO_2 + CH_3OH \rightarrow P_2Pd^{II}\text{=NPh} + CO + 2\ H_2O \tag{1c}$$
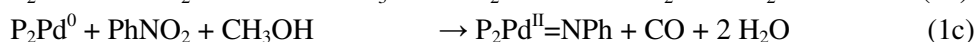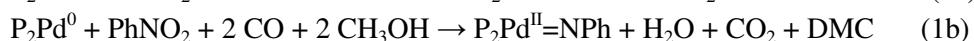
In order for these reactions to be catalytic in palladium, the P_2Pd^{II}=NPh complex must be reduced to P_2Pd^0, which can proceed as described by Equations 2a–c. This would then explain the formation of all aryl contain reduction products of

nitrobenzene; MPC (2a), aniline (2b), and Azoxy (2c). DPU formation is a modified version of Equation 2a ($PhNH_2$ instead of CH_3OH), and Azo formation can be seen as a modified version of Equation 2c (PhNO instead of $PhNO_2$), or may be the result of a further deoxygenation of azoxybenzene.

$$P_2Pd^{II}=NPh + CO + CH_3OH \quad \rightarrow P_2Pd^0 + MPC \qquad\qquad (2a)$$
$$P_2Pd^{II}=NPh + CO + 2\ CH_3OH \quad \rightarrow P_2Pd^0 + PhNH_2 + DMC \qquad (2b)$$
$$P_2Pd^{II}=NPh + CO + PhNO_2 \quad \rightarrow P_2Pd^0 + Azoxy + CO_2 \qquad (2c)$$
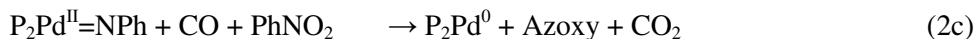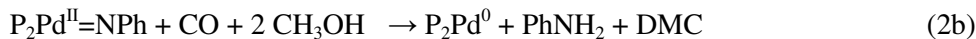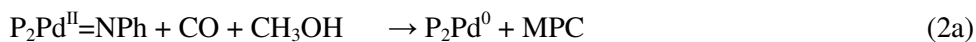
When water is formed (eq. 1b and 1c), water may replace methanol in the above reactions (eq. 2a and 2b), which will lead to phenyl carbamic acid (PhNHC(O)OH) instead of MPC in Equation 2a, or to methyl hydrogen carbonate ($CH_3OC(O)OH$) instead of DMC in Equation 2b; both are instable products and will readily decompose into $PhNH_2/CO_2$ and CH_3OH/CO_2 respectively. In both cases, this thus leads to the same stoichiometry, as is shown by Equation 2d.

$$P_2Pd^{II}=NPh + CO + H_2O \quad \rightarrow \quad P_2Pd^0 + PhNH_2 + CO_2 \qquad (2d)$$
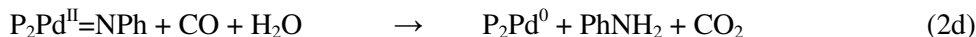
A combination of the half–reactions that oxidize Pd^0 to Pd^{II} (eqs. 1) with the half–reactions that reduce Pd^{II} to Pd^0 (eqs. 2), leads to the overall possible stoichiometries described in Chapter 3.[39] This allows the construction of a relatively simple and unifying catalytic scheme, rationalizing the formation of all methanol oxidation products and all nitrobenzene reduction products (Scheme 4.6).
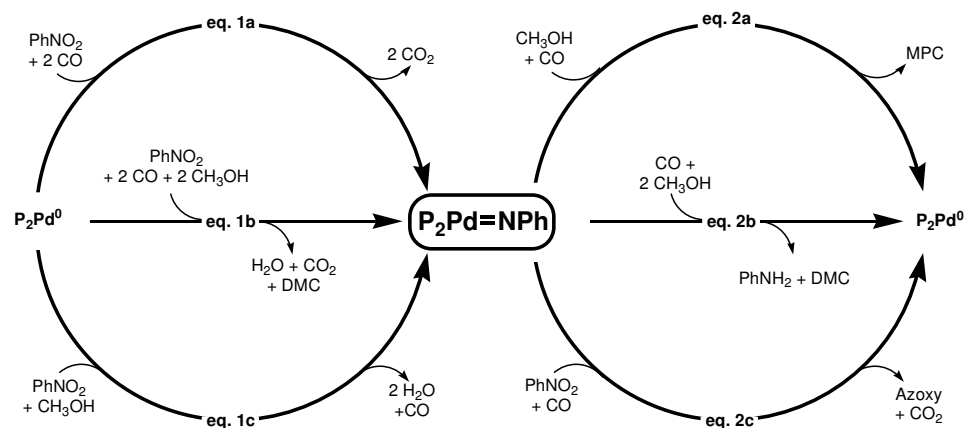
Scheme 4.6. Proposed reaction scheme for the catalytic processes in the P_2Pd-catalyzed carbonylation of nitrobenzene in methanol.

4.3.2. Nitrobenzene de–oxygenation mechanisms leading to a P$_2$Pd^{II}=NPh complex

4.3.2.1 *MPC production* via *Pd–imido complex* vs. *palladacyclic complex*

In the proposed reaction scheme condensed in Scheme 4.6, the formation of the nitrobenzene carbonylation products (MPC and DPU) does not require the palladacyclic intermediate shown in Figure 4.2 (i.e. (**II**) when L3X is the supporting ligand). However, the presence and involvement of such a species can not be excluded based on the above constructed hypothesis alone. A mechanistic pathway towards MPC that involves the palladium–imido complex (eq. 1a and 2a) cannot easily be distinguished from a mechanism involving the palladacyclic complex (eq. 3a and 3b): both amount to the same net stoichiometry as given by Equation 3c.

$$P_2Pd^0 + PhNO_2 + 3\ CO \quad\quad \rightarrow \quad\quad \text{‘}P_2\text{–palladacycle’} + CO_2 \quad\quad\quad (3a)$$
$$\text{‘}P_2\text{–palladacycle’} + CH_3OH \quad \rightarrow \quad\quad P_2Pd^0 + MPC + CO_2 \quad\quad\quad (3b)$$
$$PhNO_2 + 3\ CO + CH_3OH \quad\quad \rightarrow \quad\quad MPC + 2\ CO_2 \quad\quad\quad\quad\quad (3c)$$
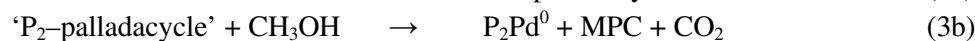
It is thus useful to elaborate on the molecular mechanistic basis underlying the proposed nitrobenzene deoxygenation pathways given in Equations 1a–c, and compare these with a possible deoxygenation pathway involving a palladacyclic complex (eq. 3a). Especially a comparison between the related deoxygenation pathways 1a and 3a (using only CO as deoxygenating reagent) will shed light on the likelihood of both pathways.

4.3.2.2 *Proposed PhNO$_2$ deoxygenation pathways; CO–only*

The commonly proposed pathway to reduce nitrobenzene with CO alone (see Scheme 4.7) when 1,10–phenanthroline is the supporting ligand, leads to the palladacycle ‘phen–**C7**’ (i.e. (**I**)) *via* the pathway **C1**→**C2**→**C3**→**C4**→**C7**. It is generally proposed that palladacycle ‘phen–**C7**’ is the direct precursor for the formation of isocyanates and carbamates.[7, 16, 18, 20, 28, 29]

The central thesis as established from the present work using bidentate diarylphosphane ligands (as P$_2$ in Scheme 4.7) in palladium-catalyzed nitrobenzene carbonylation, is that not only when methanol functions as deoxygenation agent, but also when the ‘CO–only’ deoxygenation pathway is

138

followed, the proposed Pd–imido complex **C5** is the most relevant intermediate instead of the palladacycle **C7**. The imido complex **C5** is not only necessary for a rational coupling of methanol oxidation chemistry with nitrobenzene reduction chemistry, but it is also a likely intermediate for the competing production of MPC, DPU, $PhNH_2$, and Azo(xy)benzene.
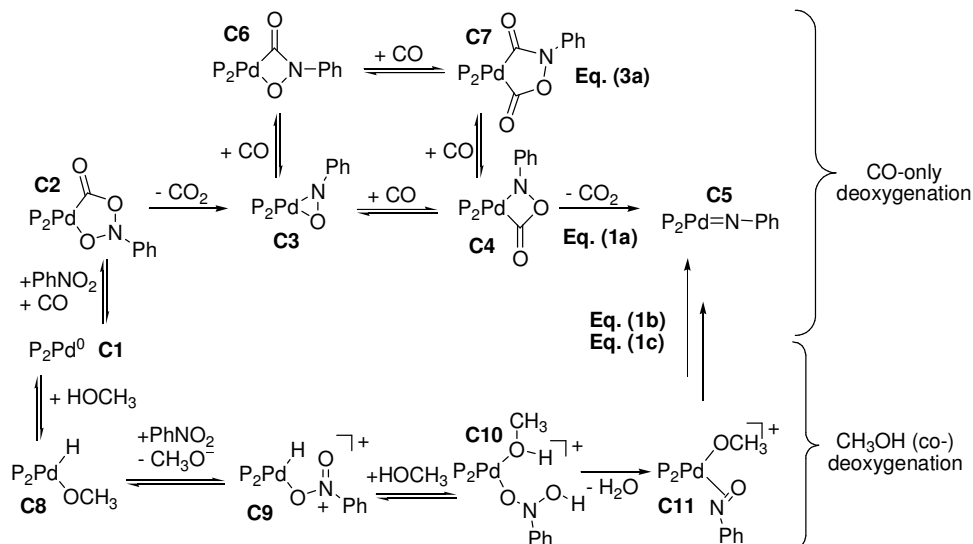
Scheme 4.7. Working hypothesis for the formation the palladacyclic intermediate (top) and the Pd–imido intermediate (centre and bottom), in the reduction of nitrobenzene.

In Scheme 4.7, the current understanding of the 'CO–only' deoxygenation pathway is summarized, including the new findings based on the NMR, ESI–MS and GLC–MS studies on the fate of a L3X–palladacycle complex (i.e., **C7** in Scheme 4.7). The first step towards the imido complex **C5** during actual catalysis is thought to involve oxidation of P_2Pd^0 (**C1**) to give species **C2**, by an oxidative coupling of CO and nitrobenzene at P_2Pd^0. Irreversible CO_2 extrusion will then lead to species **C3**, while this species under high CO pressure (carbonylation conditions) is in equilibrium with the interconvertible species, **C4**, **C6**, and **C7** *via* a series of reversible CO insertions/de-insertions (see also Scheme 4.4). In fact, it is a quite general phenomenon that in palladium-catalyzed carbonylations, e.g. of alkenes, alkynes, and alcohols, reversible carbonylation steps are involved. Escape from these equilibria can only occur by irreversible product-forming steps.[61]

139

The experimental studies and DFT calculations described above indicate that diphosphane–based palladacyclic complexes of the **C7**–type are considerably less stable than the corresponding phen–palladacyclic complexes; decarbo**n**ylation of the P_2–palladacyclic complexes takes place even at room temperature. Contrary to the initial expectations, CO_2 extrusion from the P_2-**C7** complex does not occur to a significant extent, apparently as a consequence of a higher activation barrier than decarbo**n**ylations to **C4** and/or **C6**. The CO_2 extrusion from the four-membered L3X–palladacycle **C4** to give Pd–imido species **C5** on the other hand, appears to be kinetically favourable as indicated by the NMR experiments showing an overall fast decomposition of **C7**, *via* **C4** to the several 'NPh' derived products. Only some 10% of the originally present 'NPh' fragment of the starting palladacycle in the ligand exchange experiments can be accounted for by specifically identified products, such as L3X=NPh, aniline, nitrosobenzene and phenyl isocyanate, but some 90% must thus have ended up in a variety other (possibly oligo–) aromatic compounds under the prevailing reaction conditions, with the concomitant appearance of neutral $[Pd^0(L3X)_2]$ species.

Apparently, the barrier for **C7** decarboxylation is significantly higher than the barrier for **C7** decarbonylation, thus preventing this palladacycle from being an important product-releasing species to the nitrobenzene carbonylation products MPC and DPU. In this respect, diphosphane–based catalysts could deviate from phen–based catalyst; decarboxylation of 'phen–**C7**' (i.e., complex (**I**)) has been proposed as the route to isocyanates/carbamates.[7, 16, 18, 20, 28, 29] The relative importance of decarbo**x**ylation *versus* decarbo**n**ylation of **C7** under actual carbonylation conditions will depend on the type of ligand applied in the catalyst, and on the relative activation barriers for these two processes. As discussed above, the combination of using diphosphane ligands and relatively mild reaction temperatures, likely causes the decarbo**x**ylation process not being able to compete with the lower barrier decarbo**n**ylation process, but it can, of course, not be excluded that at certain elevated temperatures and certain applied conditions the higher barrier process may also come into play. Under these circumstances an additional channel for production of carbamates will thus be opened. With diphosphanes as supporting ligands, formation of **C7** (see equations 3a,b) is, however, unlikely being a prerequisite for the formation of phenyl isocyanate or its derivative MPC. In fact, it was shown that a pre-synthesized 'Pd=NPh'

species, supported by the bpap ligand, reacts under mild conditions with CO and methanol to give the corresponding carbamate.

4.3.2.3 Proposed PhNO$_2$ deoxygenation pathways; CH$_3$OH (co–) reduction

The reduction of nitrobenzene can also be achieved by H–atoms from methanol, eventually leading to Equations (1b) and (1c). This transfer hydrogenation process most probably involves palladium hydride chemistry, without involvement of 'free' H$_2$ as is shown at the bottom of Scheme 4.7. The proposed mechanistic pathways for these stoichiometries have been described in Chapter 3,[39] and will be the focus of Chapter 5. For present purposes, it suffices to note that both deoxygenation pathways involving CH$_3$OH (eq. 1b and 1c) eventually will form *only* the imido intermediate of the **C5** type; so without any involvement of palladacyclic complexes such as **C7**.

Thus the catalytic and organometallic data presented in this chapter all point towards the P$_2$Pd^{II}=NPh complex **C5** as the most likely intermediate, not only as a key species to connect reduction of nitrobenzene with oxidation of methanol, but also as an important intermediate in the genesis of *all* the 'PhN' containing nitrobenzene reduction products, including carbonylation products.

The 5–membered palladacyclic compound **C7** on the other hand, most likely is not a significant MPC/DPU product releasing species. Instead, **C7** is thought to be part of several interconvertible (± CO) palladacycles (**C3**, **C4**, **C6**) that together act as temporary reservoir for the organic 'PhN' group. This formally fully reduced nitrobenzene fragment only escapes the reservoir species by the irreversible CO$_2$ extrusion from **C4** to form the imido-intermediate **C5**, from which the formation of all the nitrobenzene reduction products can be rationalized, including MPC and DPU.

4.3.3. Ligands effects in the reaction of P$_2$Pd^{II}=NPh

4.3.3.1 Azo(xy) formation vs. carbonylation/hydrogenation

The influence of the ligand structure on the nitrobenzene deoxygenation pathway has already been discussed in Chapter 3;[39] here the focus lies on the influence of the ligand structure on the subsequent reactivity of the P$_2$Pd–imido complex.

From the current mechanistic understanding summarized in Scheme 4.6, it follows that once the P_2Pd^{II}=NPh intermediate is formed, there is a competition between three different reactions: carbonylation (2a), hydrogenation (2b) and the coupling reaction (2c). The results described in Section 4.2.3.1 show that the selectivity for Azoxy depends on the concentration of nitrobenzene. This is in accordance with a mechanism in which nitrobenzene and methanol compete for a reaction with the same Pd–imido intermediate. This scheme also rationalizes the observation that an increase in CO pressure results in increasing contributions of carbonylation *and* hydrogenation reactions of nitrobenzene at the cost of the Azo(xy) forming coupling reactions, in agreement with the proposal that CO competes with nitrobenzene for reaction with the same Pd–imido intermediate.

When enlarging the bite-angle of the ligand considerably more Azoxy coupling products are formed (from 6% for L3 to 32% for L4, Table 1). When the ligand L4 is made more rigid (L4X), even more coupling products are produced (73%). This suggests that the steric property of the catalyst complex in the plane of coordination is an important parameter in determining the fate of the 'PhN' moiety. This effect bears resemblance with the observed strongly increased rate of the reductive elimination due to larger bite–angle P_2 ligands at a P_2Pd^{II} centre carrying two organic anionic groups.[44, 62-65] In the present system, the reductive elimination of azoxy– or azo– benzene from a $[P_2Pd^{II}$=NPh(PhNO$_2$ / PhNO] moiety is apparently accelerated by enforcing close contact at the Pd centre, between the imido group and nitro– or nitroso group and therefore simultaneously forming azo(xy) benzene and a 'P_2Pd=O' species.[66] The latter 'Pd=O' complex can enter subsequent catalytic processes, such as carbomethoxylation (*via* protonation by methanol) or carbonylative de-oxygenation of nitrobenzene (by oxidation of CO).[39] It must, however, be noted that in the ligand exchange experiments described in section 4.2.4.3, most of which were carried out in nitrobenzene as the solvent, no azo(xy) benzene could be observed as a 'NPh' derived product during the decomposition of palladacycles: obviously, its formation is still an activated process, that does not occur to any appreciable extent under the low temperature conditions applied in these experiments.

The increased relative rate of azo(xy)benzene formation cannot, however, be purely steric in origin as the presence of electron–donating methoxy groups, *both*

in the ortho– *and* in the *para*–positions of the phenyl rings, significantly suppresses the coupling reaction (from 32% for L4 to 7% for pMeO–L4). A similar effect is observed when comparing L3 with pMeO–L3 (6% *vs*. 1%).

The bite angle of the ligand can also have an effect on the basicity of the imido–nitrogen of the corresponding P_2Pd^{II}=NPh complex. Palladium complexes of P_2-ligands with a C3–backbone are characterized by a P–Pd–P angle close to 90°, which is ideal for maximal orbital overlap. In complexes of P_2-ligands with a C4–backbone, this P–Pd–P angle typically is around 94°.[45] In these complexes there will thus be less orbital overlap, which in turn hampers the flow of electrons from the aryl rings to palladium. This is indeed reflected in the DFT–calculated basicity of the imido–nitrogen atom, which is higher for (L3X)Pd=NPh than for (L4)Pd=NPh. Thus, for electronic reasons (partially dictated by the steric properties of the ligand backbone), protonation (also leading to carbonylation, *vide supra*), is more easily achieved in the case of the L3–type ligands, whereas the 'disproportionation' reaction is relatively facilitated by employing L4–type ligands in the catalytic system.

4.3.3.2 Carbonylation vs. hydrogenation

In general, more carbonylation products (MPC, DPU) are formed relative to hydrogenation products ($PhNH_2$, DPU) when equipping the ligand with *ortho*–methoxy groups or when using ligands with a smaller bite angle.

The effect of the *ortho*–methoxy substitution on the product distribution can be rationalized with the understanding of this part of the mechanism as shown in Scheme 4.8. First, the imido nitrogen can be protonated by a CH_3OH molecule that is approaching the Pd–centre *via* the sterically not so demanding equatorial positions (see also Figure 4.19), thus forming **C12**. As this species does not have any open sites in the equatorial positions, a second CH_3OH molecule must approach the Pd–centre *via* its axial positions, resulting in the formation of aniline and the $P_2Pd^{II}(OCH_3)_2$ complex **C14**. The *o*–MeO groups will hamper this second protonation step as they shield the axial positions of Pd.[40, 67, 68] Hence, less $PhNH_2$ is formed. MPC is formed instead by an associative displacement of the CH_3O^- anion in **C12** by a smaller and neutral CO molecule, followed by

nucleophilic attack of nearby CH_3O^- on coordinated CO (giving **C13**) and reductive elimination to yield MPC and P_2Pd^0 (**C1**).
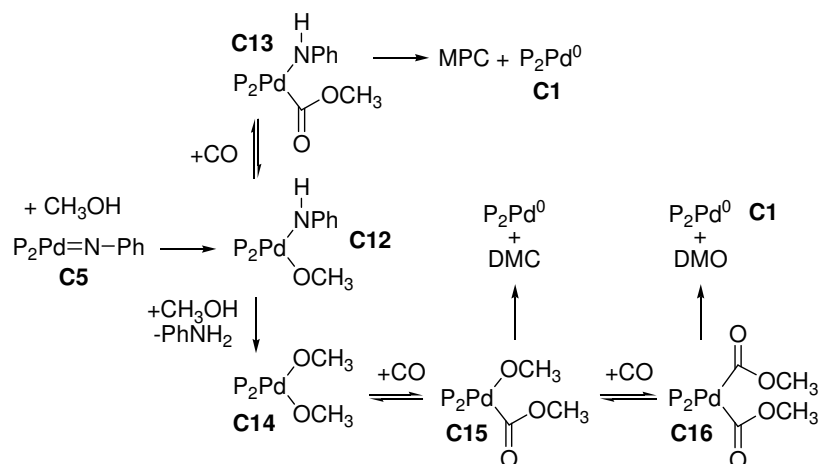
Scheme 4.8. Mechanistic scheme showing the related production of MPC and $PhNH_2$ (+DMC/DMO)

The effect of the larger ligand bite–angle giving a lower amount of carbonylation product relative to the hydrogenation product could be the consequence of a relatively better accessibility at P_2Pd^{II} by a charge–polarized methanol (CH_3O^- $\cdots H^+$) molecule at the fifth and sixth coordination site, relative to a neutral CO molecule, which would lead to a simultaneous coordination of an anionic CH_3O^- and protonation at PhN^{2-} to give **C14**, rather than **C13**.

An electronic effect may play an additional role in the relative weight of **C12→C13** (carbonylation) *vs*. **C12→C14** (hydrogenation). The difference in orbital overlap (between Pd and the P–donor atoms) caused by the L3 *vs*. L4 ligands can render the palladium centre in L4–complexes more electrophilic than in L3–complexes and therefore more susceptible by attack by methanol, relative to CO.

It is important to note that when methanol is replaced by H_2O (formed *in situ* during $PhNO_2$ de–oxygenation with CH_3OH) in the above processes, both pathways shown in Scheme 4.8 will lead to $PhNH_2$ and CO_2 as the carbonylation product instead of MPC or DMC/DMO. It was shown in Chapter 3 that this

readily occurs when using L3–ligands but much less so with L4–ligands,[39] which is consistent with the fact that catalysts equipped with the L4 ligand also produce relative less MPC/DPU.

Summarizing, catalysts with L3–ligands follow mostly (and with the oMeO–functionality almost only) the reaction sequence **C5→C12⇌C13→C1** (with CH_3OH to give MPC, *or* with H_2O to give $PhNH_2$ and CO_2), while catalysts supported with L4–ligands react for a larger portion *via* the sequence **C5→C12→C14⇌C15(⇌C16)→C1**.

4.3.4. Effects of the acidity

Interestingly, the effect of making the reaction medium more acidic is radically different for the two catalytic systems based on Pd^{II}(L4X) or Pd^{II}(o–MeO–L3X). In the reaction catalyzed with Pd^{II}(L4X), an increase in the acidity results in suppression of the coupling reaction in favor of the hydrogenation and carbonylation reactions. This is in agreement with the hypothesis that methanol and nitrobenzene compete for reaction with the imido intermediate; making the reaction more acidic facilitates the protonation of P_2Pd^{II}=NPh and thus favors the hydrogenation *and* carbonylation reactions. That the hydrogenation is promoted more than the carbonylation reaction can then be ascribed to the facilitation of the second protonation (i.e., reaction of CH_3OH with **C12** in Scheme 4.8).

On the other hand, the selectivity of the catalytic system based on Pd^{II}(o–MeO–L3X) is far less affected by the addition of acid. This observation is easily understood when realizing that with this specific catalyst the imido–intermediate is *already* predominantly involved in the carbonylation reaction following the sequence **C5→C12⇌C13→C1** route shown in Scheme 4.8. That is, the oMeO–moieties of this ligand shield the palladium centre in the catalyst, thus hampering the second protonation by methanol (from **C12** to **C14**).

4.4. Summary and conclusions

Nitrobenzene reduction in a CO/CH_3OH environment is catalyzed by Pd–diphosphane complexes. The fully deoxygenated nitrobenzene 'PhN' moiety can end up in carbonylation products, hydrogenation products and coupling products. It was shown that the selectivity for these three reactions can be altered by

145

adjusting the steric and electronic properties of the ligand in the catalyst, by changing the concentration of CO or $PhNO_2$, and by varying the acidity of the reaction medium. These findings could be rationalized by a relatively simple mechanistic scheme, that is centered around the palladium–imido complex 'P_2Pd^{II}=NPh' as the central product-releasing intermediate (see also Chapter 3).

As an alternative product-releasing intermediate for the carbonylation products MPC and DPU, the palladacycle '$L_2PdC(O)N(Ph)OC(O)$' (see Figure 4.2a) was considered, which is commonly proposed as product-releasing species when L_2 is the N–donor ligand 1,10–phenanthroline. It was concluded from NMR studies, GLC(–MS), and ESI–MS analysis, that 5–membered 'L3X–palladacycle' (**II**) – obtained by a ligand exchange reaction of 'phen–palladacycle' (**I**) with diphosphane ligand L3X– readily decomposes under mild conditions *via* a reversible decarbonylation reaction to give L3X–palladacycles (**III**) and/or (**IV**). This clearly suggests that the barrier for decarbo**n**ylation of palladacycle (**II**) must be significantly lower than that of decarbo**x**ylation of this species. The low stability of a diphosphane–palladacycle relative to a phen–palladacycle is mainly attributed to increased steric constraints imposed on the palladacycle by the diphosphane ligands. This is supported by DFT calculations.

Decomposition of palladacycle (**III**) by loss of CO_2 would give the thus far elusively palladium–imido species (L3X)Pd^{II}=NPh, which in the presence of excess of L3X under the mild ligand-exchange conditions and in the absence of CO rapidly is converted to [$Pd^0(L3X)_2$] and a manifold of aromatic compounds. Aniline and nitrosobenzene account for only about 10% of the aromatic compounds, while mere traces of phenyl isocyanate were observed.

Evidence for a '(L3X)Pd=NPh' type of intermediate under real carbonylation conditions was obtained from *in situ* trapping experiments with cyclohexene. Additional proof for the existence of a P_2Pd–imido species and its reactivity comes from the synthesis of the model complex (bpap)Pd^{II}=NMes, as observed by ^{31}P–NMR and ESI–MS. This (bpap)Pd^{II}=NMes complex was shown to react with CO and methanol to give methyl mesityl carbamate, already under mild conditions.

~ PhD Thesis: Towards a Sustainable Synthesis of Aromatic Isocyanates ~

Based on the presented organometallic data, it is proposed that under real carbonylation conditions (relatively high CO pressure and elevated temperatures), the existing palladacyclic complexes (**C3**, **C4**, **C6**, and **C7** in Scheme 4.7) are engaged in reversible carbonylation/decarbonylation reactions. Irreversible product release from this set of –presumably equilibrated– palladacycles can occur by low–barrier loss of CO_2 from intermediate **C4** to give the highly reactive P_2Pd^{II}=NPh intermediate (**C5**). Such a P_2Pd^{II}=NPh species is not only able to release reduction products like aniline (by protonation) and Azo(xy) (by coupling with nitrosobenzene or nitrobenzene), but also to release the carbonylation products MPC and DPU (by reaction with CO and methanol or aniline, respectively).

The combined catalytic and organometallic data thus all point strongly to a P_2Pd^{II}=NPh complex as the *sole most probable product releasing* intermediate species in the Pd/diphosphane catalyzed reduction reactions of nitrobenzene in a methanol/CO environment.

4.5. Experimental section

4.5.1. General remarks

All ligands were generously provided by Shell Global Solutions Amsterdam b.v., where they were synthesized according to literature procedures.[51, 56, 69-77] All other solids were purchased from Acros organics and used as received. Methanol, nitrobenzene and aniline were all of analytical reagent purity, and were distilled under an argon atmosphere over the appropriate drying agent.[78] After the distillation, these liquids were saturated with argon. It was ensured that no water was present using an analytical reaction with trimethylorthoformate according to a modified literature procedure[79] (see below and also SI). Carbon monoxide (> 99% pure)[80] was purchased from Linde gas Benelux B.V. and used as received.

^{1}H–, ^{31}P{^{1}H}–, and ^{13}C–NMR spectra were recorded on a Bruker DPX300 (300 MHz) or a Bruker DMX400 (400 MHz) machine. Chemical shifts are recorded in δ (parts per million) relative to the solvent peak (^{1}H– and ^{13}C–NMR) or relative to phosphoric acid as external standard (^{31}P{^{1}H}–NMR). IR–spectra were recorded with 4 cm^{-1} resolution on a Perkin Elmer Paragon 1000 FT–IR fitted with a Golden Gate Diamond ATR. Elemental analyses were performed using a Perking Elmer 2400 Series II CHNS/O analyzer. A Finnigan Aqua Mass Spectrometer (MS) with electro spray ionization (ESI) was used to record mass spectra. Sample introduction was achieved through a Dionex ASI–100 automated sample injector with the eluent CH_3CN flowing at 0.2 ml/min. The voltage of the capillary and the voltage for the aquamax were set at 3 kV and 20 V respectively. High pressure catalysis experiments were conducted in stainless steel autoclaves (100 ml) equipped with two inlet/outlet valves, a burst disc, a pressure sensor, and a thermocouple. The autoclaves were heated by a HEL$^©$ polyBLOCK electrical heating system. Temperatures and pressures where measured with probes connected to a computer interface making it possible to record these parameters throughout the course of the reaction. GLC–MS measurements were performed on a Hewlett Packard series 2 type 5890 gas chromatograph equipped with a Hewlett Packard 5971 mass

147

selective detector. Details of the catalytic experiments and analysis have been described in Chapter 3.[39]

4.5.2. General procedure DFT studies

Calculations were done with the SPARTAN '04 package (Wavefunction, Inc; www.wavefun.com), using density functional theory (DFT)[81, 82] with the Becke and Perdew (BP) functional.[83, 84] Geometry optimizations were carried out using Pople's 6–31G* (d,p) for H, C, O, and P atoms[85] and the LANL2DZ effective core potential for palladium.[86-88] All of the geometrical parameters were fully optimized, and all of the structures located on the PESs were characterized as minima. No constraints to bonds, angles, or dihedral angles were applied in the calculations, and all atoms were free to be optimized.

4.5.3. Starting geometries for DFT studies

Initial atomic coordinates were extracted from Pd(L3)Cl$_2$ (CSD refcode DPPPDC)[89] and Pd(L4)Cl$_2$ (CSD refcode RINZOD).[90] The chloride anions were manually deleted and the rest of the molecule was 'frozen' using the 'freeze centre' option in Spartan. From these geometries, the diphosphane ligands were adjusted to L3X and oMeOL3X (starting from 'Pd(L3)'), and pMeOL4 and L4X (starting from 'Pd(L4)'), and a geometry optimization was performed using molecular mechanics (MMFF), while the 'frozen atoms' remained frozen. All atoms in these 'P$_2$Pd' complexes were then 'frozen', and used to generate the P$_2$Pd(CO)$_2$, P$_2$Pd–palladacycle, and P$_2$Pd=NPh complexes reported in this study. For the P$_2$Pd(CO)$_2$ complexes, two CO ligands were added to Pd in the appropriate 'P$_2$Pd' complex, the PPPd–PdCC angle was fixed to 90°, and a geometry optimization was performed using molecular mechanics (MMFF). All constraints were then released, and the DFT geometry optimization was started as described above. For the P$_2$Pd–palladacycle complexes, a planar 'C(O)N(Ph)OC(O)' fragment was added to Pd, the PPPd – PdCC angle was fixed to 0°, and a geometry optimization was performed using molecular mechanics (MMFF). All constraints were then released, and the DFT geometry optimization was started as described above. For the P$_2$Pd=NPh complexes, a 'NPh' ligand was added to Pd, the Pd–N–C angle was set to 180°, the P–Pd–N angles were set so that the imido–N was positioned in the plane of coordination and exactly in between the two P–atoms. A geometry optimization was then performed using molecular mechanics (MMFF). All constraints were then released, and the DFT geometry optimization was started as described above.

4.5.4. NMR kinetic measurements

9.00 mg (20 μmol) of 'phen–palladacycle'[16] (see Figure 4.2a) was weighed into an NMR tube and put under argon. In another tube, the appropriate amount of phosphane ligand was dissolved in 1 ml (d^5–)nitrobenzene under an argon atmosphere. Of this solution, 0.8 ml was added to the 'phen–palladacycle' complex using a 1 ml syringe, which was dry and flushed with argon. The thus obtained yellow suspention (20 mM 'phen–palladacycle') was thoroughly mixed using a vortex mixer and measured. After the first measurements, the reaction mixture was carefully heated to about 60 °C, resulting in a clear yellow–orange solution. This solutions were monitored with ^{1}H– and ^{31}P{^{1}H}–NMR spectroscopy, over a period of fourteen hours. For the proton measurements, the number of free inductive decays (FIDs) was 16 and for the phosphorus NMR spectra the number of FIDs was 40. The same procedure was applied for the experiment under a CO atmosphere, but nitrobenzene was first saturated with CO gas, the NMR–tube was put under a CO atmosphere and the 1 ml syringe was flushed with CO.

4.5.5. Synthesis of 2,4,6–trimethylphenyl azide (N$_3$Mes)

N$_3$Mes was obtained in 86% yield (9.58 g) as clear colorless liquid from 2,4,6–trimethylaniline following a literature procedure.[91, 92] GLC–MS: t$_R$ = 16.96 min, m/z found (calc): 161 (161.10)

$[N_3Mes]^+$, 133 (133.09) $[NMes]^+$, 119 (119.09) $[Mes]^+$, 104 (104.06) $[Mes–CH_3]^+$. ^1H–NMR (300 MHz, CDCl$_3$, 25 °C) δ = 2.45 (s, 3H, p–CH_3), 2.52 (s, 6H, o–CH_3), 6.99 (s, 2H, m–H) ppm; ^{13}C–NMR (75 MHz, CDCl$_3$, 25 °C) δ = 17.91 (s, o–CH_3), 20.59 (s, p–CH_3), 129.45 (s, N$_3$CC(CH3)CH) 131.72 (s, N$_3$CC(CH3), 134.36 (s, N$_3$CC(CH3)CHC(CH3)), 135.19 (s, N$_3$$C$) ppm. IR (neat, cm^{-1}): 2919 (weak, CH), 2114 (very strong, N$_3$), 1477 (strong, Ph), 1278 (strong, N$_3$ (organic)), 852 (strong, Ph C=C).

4.5.6. Synthesis of Pd(bpap)(dba)

In 15 ml toluene were successively dissolved 112.2 mg (0.12 mmol) Pd$_2$(dba)$_3$ (dba = dibenzylideneacetone) and 118.6 mg (0.25 mmol) of a rac ($\alpha\alpha/\beta\beta$) and $meso$ (α/β) diastereoisomeric mixture of 1,3–bis(1,3,5,7–tetramethyl–4,6,8–trioxa–2–phosphaneamantane)propane (bpap). The resulting dark red solution was stirred for one hour, while shielding the reaction vessel from light with tin foil. After the solution turned green, it was filtered over a 0.45 μm micro–filter. Solvent was removed *in vacuo* from the yellow–gold colored filtrate. The residue was dissolved in 1 ml of dichloromethane followed by the addition of several milliliters of n–hexane. Within minutes a precipitate was obtained. The solid was collected by filtration dried *in vacuo*, and analyzed as Pd(bpap)(dba) · toluene (120 mg, 54%). Elemental analysis calcd. for C$_{40}$H$_{52}$O$_7$P$_2$Pd · Toluene (Mw = 905.34): C, 62.35; H, 6.68%. Found: C, 62.44; H, 6.67%. MS (ESI) found (calc): m/z 812.85 (812.22) [Pd(bpap)(dba)]$^+$. ^1H–NMR (300 MHz, CDCl$_3$, 25 °C) δ = 1.00–2.50 (m, 38H, bpap), 7.09 (d, 2H, –C(=O)CH=CH–Ph), 7.34 (d, 4H, o–H), 7.62 (m, 6H, m/p–H), 7.75 (d, 2H, –C(=O)CH=CH –Ph) ppm; $^{31}P\{^1H\}$–NMR (121 MHz, CDCl$_3$, 25 °C) δ = 4.06 (s, $meso$), –0.63 (s, rac) ppm. IR (neat, cm^{-1}): 2978 (weak, CH$_2$), 1574 (medium, cage), 1436 (strong, cage), 1286 (string, C–O), 1232 (strong, C–O), 1031 (stong, C–O–C), 750 (very strong, P–C).

4.5.7. *In situ* synthesis of (bpap)Pd=NMes

3.89 mg (4.3 μmol) of Pd(bpap)(dba)·toluene was weighed into an NMR tube and put under argon. The complex was dissolved in 0.3 ml dry and degassed d^8–toluene, which was added with a dry and argon flushed 1 ml syringe. In a similar fashion, 0.3 ml N$_3$Mes was added, which was saturated with argon prior to use. The resulting clear solution was heated to 50 °C in about 45 minutes, where after the solution was heated to 100 °C, also in about 45 minutes. The reaction mixture was then allowed to cool to laboratory temperature. The whole process was monitored with ^1H– and $^{31}P\{^1H\}$–NMR spectroscopy, and after cooling the reaction mixture was analyzed with ESI–MS.

References

[1]   www.gem-chem.net/capacity.html, **November 2011**
[2]   A. J. Ryan, J. L. Stanford, *in: G. Allen, J.C. Bevington (eds.), Comprehensive Polymer Science, Vol. 5*, Pergamon, New York, **1989**.
[3]   K. Weisermel, H. J. Arpe, *Industrielle Organische Chemie*, VCH Verslagsgesellschaft GmbH, Weinheim, Germany, **1988**.
[4]   H. Ulrich, *Ullmann's Encyclopedia of Industrial Chemistry, Vol. A14*, VCH publishers, New York, **1989**.
[5]   *Registry of Toxic Effects of Chemical Substances (RTECS, online database)*, United States Department of Health and Human Services (National Toxicology Information, National Library of Medicine), Bethesda, MD, **1993**.
[6]   R.C. Weast (Ed.), *Handbook of Chemistry and Physics*, D-110, 58 ed., CRC Press Inc., Cleveland, **1977-1978**.
[7]   F. Paul, *Coord. Chem. Rev.* **2000**, *203*, 269.
[8]   F. Ragaini, *Dalton Trans.* **2009**, 6251.
[9]   E. Drent, P. W. N. M. van Leeuwen, EU 0086281A1, **1982**.
[10]   E. Drent, EU 224292, **1987**.
[11]   E. Drent, EU 0231045A2, **1987**.

[12]   E. Drent, *Pure Appl. Chem.* **1990**, *62*, 661.

[13]   A. Bontempi, E. Alessio, G. Chanos, G. Mestroni, *J. Mol. Catal.* **1987**, *42*, 67.

[14]   S. Cenini, F. Ragaini, M. Pizzotti, F. Porta, G. Mestroni, E. Alessio, *J. Mol. Catal.* **1991**, *64*, 179.

[15]   R. Santi, A. M. Romano, F. Panella, G. Mestroni, A. Sessanti, A. S. o Santi, *J. Mol. Catal. A-Chem.* **1999**, *144*, 41.

[16]   P. Leconte, F. Metz, A. Mortreux, J. A. Osborn, F. Paul, F. Petit, A. Pillot, *J. Chem. Soc.-Chem. Commun.* **1990**, 1616.

[17]   P. Wehman, V. E. Kaasjager, W. G. J. de Lange, F. Hartl, P. C. J. Kamer, P. W. N. M. van Leeuwen, J. Fraanje, K. Goubitz, *Organometallics* **1995**, *14*, 3751.

[18]   P. Wehman, G. C. Dol, E. R. Moorman, P. C. J. Kamer, P. W. N. M. van Leeuwen, J. Fraanje, K. Goubitz, *Organometallics* **1994**, *13*, 4856.

[19]   P. Wehman, PhD thesis, University of Amsterdam (UvA) **1995**.

[20]   P. Wehman, L. Borst, P. C. J. Kamer, P. W. N. M. van Leeuwen, *J. Mol. Catal. A-Chem.* **1996**, *112*, 23.

[21]   F. Ragaini, C. Cognolato, M. Gasperini, S. Cenini, *Angew. Chem.* **2003**, *42*, 2886.

[22]   F. Ragaini, M. Gasperini, S. Cenini, *Adv. Synth. Catal.* **2004**, *346*, 63.

[23]   E. Drent, P. E. Prillwitz, EU ZA8609251 (A), **1985**.

[24]   J. H. Grate, D. R. Hamm, D. H. Valentine, US 4.603.216, **1986**.

[25]   P. Wehman, R. E. Rulke, V. E. Kaasjager, P. C. J. Kamer, H. Kooijman, A. L. Spek, C. J. Elsevier, K. Vrieze, P. W. N. M. van Leeuwen, *J. Chem. Soc.-Chem. Commun.* **1995**, 331.

[26]   P. Wehman, H. M. A. van Donge, A. Hagos, P. C. J. Kamer, P. W. N. M. van Leeuwen, *J. Organomet. Chem.* **1997**, *535*, 183.

[27]   P. Wehman, L. Borst, P. C. J. Kamer, P. W. N. M. van Leeuwen, *Chem. Ber.-Recl.* **1997**, *130*, 13.

[28]   N. Masciocchi, F. Ragaini, S. Cenini, A. Sironi, *Organometallics* **1998**, *17*, 1052.

[29]   A. S. o Santi, B. Milani, E. Zangrando, G. Mestroni, *Eur. J. Inorg. Chem.* **2000**, 2351.

[30]   K. Nomura, *J. Mol. Catal. A.* **1998**, *130*, 1.

[31]   J. E. Yanez, A. B. Rivas, J. Alvarez, M. C. Ortega, A. J. Pardey, C. Longo, R. P. Feazell, *J. Coord. Chem.* **2006**, *59*, 1719.

[32]   F. J. Weigert, *J. Org. Chem.* **1973**, *38*, 1316.

[33]   T. Kajimoto, J. Tsuji, *Bul. Chem. Soc. Jpn.* **1969**, *42*, 827.

[34]   Smolinsk.G, B. I. Feuer, *J. Org. Chem.* **1966**, *31*, 3882.

[35]   M. Akazome, T. Kondo, Y. Watanabe, *J. Org. Chem.* **1994**, *59*, 3375.

[36]   R. Waterman, G. L. Hillhouse, *J. Am. Chem. Soc.* **2008**, *130*, 12628.

[37]   R. Waterman, G. L. Hillhouse, *J. Am. Chem. Soc.* **2003**, *125*, 13350.

[38]   D. J. Mindiola, G. L. Hillhouse, *J. Am. Chem. Soc.* **2001**, *123*, 4623.

[39]   T. J. Mooibroek, L. Schoon, E. Bouwman, E. Drent, *Chem. Eur. J.* **2011**, DOI: 10.1002/chem.201100923.

[40]   T. J. Mooibroek, E. Bouwman, M. Lutz, A. L. Spek, E. Drent, *Eur. J. Inorg. Chem.* **2010**, *2*, 298.

[41]   Note that DPU can be formed by the reaction of nitrobenzene, CO and (*in situ* generated) aniline, but also by the transesterification of MPC with aniline. In both cases, aniline is formed first and DPU is thus derived from aniline.

[42]   T. J. Mooibroek, E. Bouwman, E. Drent, *Organometallics* **2011**, submitted.

[43]   When using some ligands with an ethylene backbone (not shown in the table), the conversion was very low and a significant amount of plating (Pd^0) was observed. This was the case for both pre synthesized and *in situ* prepared catalyst precursors, indicating that P$_2$Pd(OAc)$_2$ complexes with these ligands are not stable under typical reaction conditions. An additional difficulty with such ligands is that the anticipated P$_2$Pd(OAc)$_2$ catalyst precursor is not the kinetic product of the complex forming reaction. NMR studies performed with 1,2-bis(diphenylphosphane)ethane (L2) as the P$_2$ ligand indeed showed that the catalytically inactive [(L2)$_2$Pd](OAc)$_2$ is the kinetic product of complex forming

150

in methanol (see Chapter 2 and references 40 and 68). For these reasons, the results of these experiments will not be discussed.

[44]   P. Dierkes, P. W. N. M. van Leeuwen, *J. Chem. Soc. Dalton Trans.* **1999**, 1519.

[45]   T. Hayashi, M. Konishi, Y. Kobori, M. Kumada, T. Higuchi, K. Hirotsu, *J. Am. Chem. Soc.* **1984**, *106*, 158.

[46]   S. Ross, The Proton: applications to organic chemistry in *Organic Chemistry; a series of monographs, Vol. 46* (Ed.: H. H. Wasserman), Academic Press Inc., London, **1985**.

[47]   A. S. o Santi, B. Milani, G. Mestroni, E. Zangrando, L. Randaccio, *J. Organomet. Chem.* **1997**, *546*, 89.

[48]   After 180 minutes, the solution contained 17% of 'phen-palladacycle' and 83% phen (^{1}H-NMR), meaning that only 83% of the initially added palladium can end up as L3X-complex. The percentage of a specific L3X-Pd complex (relative to palladium) can thus be calculated by: $\int_{L3X-complex} / \Sigma_{\int all\ L3X-complexes} * 83\%$. Thus, the species detected with $^{31}P\{^{1}H\}$-NMR that were assigned to Pd-containing species (see also Figure A.III.2 in Appendix III) are (δ ($\int$; assignment; percentage based on Pd)): 1.0 (1.00; $Pd^0(L3X)_2$; 33%); 5.0 (0.06; 'L3X-palladacycle'; 4%); 13 - 20 (0.33; unknown Pd complexes; 22%); 24/-7 (0.32; de*carbonylated* 'L3X-palladacycle'; 21%); 35 (0.05; unknown Pd complex; 3%); $\Sigma\int$ = 1.76. The solution also contained L3X (-25 ppm, $\int$ = 0.33) and 'L3X=O' (26/-24 ppm, $\int$ = 0.30), which is ((0.33+0.30)/1.76*100% =) 26% of the initially added L3X. Hence, 74% of L3X is thus bound to palladium; this is indeed roughly one equivalent with respect to the 83% Pd-complex, computed based on ^{1}H-NMR.

[49] $\int_{0.5\ ppm}$ = 100 ($Pd^0(L3X)_2$ = 4P); $\int_{14.3+(-26.2)\ ppm}$ = 2.2 ('L3X=NPh', 2P). Hence: 2.2/(100/2+2.2)*100% = 4.2%, and 4.2% of 10 μmol (the amount of phen-palladacycle present) is ~0.4 μmol.

[50]   The estimated cone-angle in of dpap is 173° (V. Gee *et al.*, *Chem. Comm.*, **1999**, p901); compare to 155° for ($(t$-Bu$)_2$P$)_2$(CH$_2$)$_3$ in its PtCl$_2$ complex (M. Harada *et al.*, *Bull. Chem. Soc. Jpn.*, **1979**, 52, p390).

[51]   V. Gee, A. G. Orpen, H. Phetmung, P. G. Pringle, R. I. Pugh, *Chem. Commun.* **1999**, 901.

[52]   K. C. Gross, P. G. Seybold, C. M. Hadad, *Int. J. Quant. Chem.* **2002**, *90*, 445.

[53]   A. E. Reed, R. B. Weinstock, F. Weinhold, *J. Chem. Phys.* **1985**, *83*, 735.

[54]   The natural population analysis provides the most reliable indictor of charge and basicity, and is relatively basis-set independent (see reference 52 and K. B. Wiberg, P. R. Rablen, *J. Comp. Chem.* **1993**, *14*, 1504).

[55]   M. J. McGlinch, F. G. A. Stone, *Chem. Comm.* **1970**, 1265.

[56]   J. H. Downing, J. Floure, K. Heslop, M. F. Haddow, J. Hopewell, M. Lusi, H. Phetmung, A. G. Orpen, P. G. Pringle, R. I. Pugh, D. Zambrano-Williams, *Organometallics* **2008**, *27*, 3216.

[57]   The option was considered that an un-symmetric complex was formed, that may give rise to a double doublet (one around 28 ppm and one around -15 ppm) in the $^{31}P\{^{1}H\}$-NMR spectrum. This was excluded as follows. The resonances at -15.3 and -15.8 would have a coupling constant of 0.5 ppm. No such presumed coupling is observed between the resonance around 27.6 ppm and one of the smaller peaks around 27.9 or 28.0 ppm. Also, both resonances around 27.9 and 28.0 ppm are considerably smaller ($\int$ = 0.14 and 0.34 respectively, relative to 1.00 for -15.3 ppm) than the resonance around -15.82 ppm ($\int$ = 0.51).

[58]   S. Brase, C. Gil, K. Knepper, V. Zimmermann, *Angew. Chem.* **2005**, *44*, 5188.

[59]   The other peaks were of mesitylene azide (t$_R$ = 16.8 minunes (60%), m/z = 161 [M]$^+$; 133 [M-N$_2$]$^+$) and azo mesitylene (t$_R$ = 27.8 minunes (20%), m/z = 266 [M]$^+$).

[60]   J. P. Collman, M. Kubota, J. W. Hosking, *J. Am. Chem. Soc.* **1967**, *89*, 4809.

[61]   E. Drent, P. H. M. Budzelaar, *Chem. Rev.* **1996**, *96*, 663.

[62]   P. W. N. M. van Leeuwen, P. C. J. Kamer, J. N. H. Reek, P. Dierkes, *Chem. Rev.* **2000**, *100*, 2741.

[63]   R. J. van Haaren, K. Goubitz, J. Fraanje, G. P. F. van Strijkdonk, H. Oevering, B. Coussens, J. N. H. Reek, P. C. J. Kamer, P. W. N. M. van Leeuwen, *Inorg. Chem.* **2001**, *40*, 3363.
[64]   E. Zuidema, P. W. N. M. van Leeuwen, C. Bo, *Organometallics* **2005**, *24*, 3703.
[65]   M. N. Birkholz, Z. Freixa, P. W. N. M. van Leeuwen, *Chem. Soc. Rev.* **2009**, *38*, 1099.
[66]   B. Marciniec, E. Mackowska, *J. Mol. Cat.* **1989**, *51*, 41.
[67]   I. M. Angulo, E. Bouwman, M. Lutz, W. P. Mul, A. L. Spek, *Inorg. Chem.* **2001**, *40*, 2073.
[68]   A. Marson, A. B. van Oort, W. P. Mul, *Eur. J. Inorg. Chem.* **2002**, *11*, 3028.
[69]   F. Bickelhaupt, US 4874897, **1989**.
[70]   W. Eilenberg, EU 364046, **1991**.
[71]   J. A. van Doorn, US 4994592, **1991**.
[72]   R. van Ginkel, US 6548708, **2003**.
[73]   E. Drent, US 5091587, **1992**.
[74]   C. F. Hobbs, US 4120901, **1987**.
[75]   P. W. Clark, B. J. Mulraney, *J. Organomet. Chem.* **1981**, *217*, 51.
[76]   J. M. Brown, B. A. Murrer, *Tetrahedron Lett.* **1980**, *21*, 581.
[77]   R. L. Wife, A. B. van Oort, J. A. van Doorn, P. W. N. M. van Leeuwen, *Synthesis* **1983**, *1*, 71.
[78]   W. L. F. Armarego, C. L. L. Chai, *Purification of laboratory chemicals*, 5th ed., Elsevier, Amsterdam, **2003**.
[79]   J. Chen, J. S. Fritz, *Anal. Chem.* **1991**, *63*, 2016.
[80]   customer.linde.com/FIRSTspiritWeb/linde/LGNL/media/datasheets/NL-PIB-0024.pdf, **November 2011**
[81]   W. Koch, M. C. Holthausen, *A Chemist's Guide to Density Functional Theory*, 2nd ed., Wiley-VCH, Weinheim, **2000**.
[82]   K. Eichkorn, O. Treutler, H. Ohm, M. Haser, R. Ahlrichs, *Chem. Phys. Lett.* **1995**, *240*, 283.
[83]   A. D. Becke, *Phys. Rev. A* **1988**, *38*, 3098.
[84]   J. P. Perdew, *Phys. Rev. B* **1986**, *33*, 8822.
[85]   W. J. Hehre, L. Radom, P. R. van Schleyer, J. A. Pople, *Ab Initio Molecular Orbital Theory*, Wiley, New York, **1986**.
[86]   P. J. Hay, W. R. Wadt, *J. Chem. Phys.* **1985**, *82*, 270.
[87]   P. J. Hay, W. R. Wadt, *J. Chem. Phys.* **1985**, *82*, 299.
[88]   W. R. Wadt, P. J. Hay, *J. Chem. Phys.* **1985**, *82*, 284.
[89]   W. L. Steffen, G. J. Palenik, *Inorg. Chem.* **1976**, *15*, 2432.
[90]   V. D. Makhaev, Z. M. Dzhabieva, S. V. Konovalikhin, O. A. Dyachenko, G. P. Belov, *Russ. J. Coord. Chem. (Koord. Khim.)* **1996**, *22*, 598.
[91]   S. W. Kwok, J. R. Fotsing, R. J. Fraser, V. O. Rodionov, V. V. Fokin, *Org. Lett.*, *12*, 4217.
[92]   R. E. Conrow, W. D. Dean, *Org. Proc. Res. Dev.* **2008**, *12*, 1285.

~ PhD Thesis: Towards a Sustainable Synthesis of Aromatic Isocyanates ~